Table 3. Gene Expression Data of the Probe Sets in the Affymetrix Human Genome U133 Plus 2.0 Array for the Characterization of Undifferentiated Stem Cells (*Continued*)

				Flag[a]				Fold Change Versus DMC54		Fold Change Versus KhES1	
Probe Set ID	UniGene ID	Gene Title	Symbol	DMC54	DMC5403	DMC5413	KhES1	DMC5403	DMC5413	DMC5403	DMC5413
207466_at	Hs.278959	Galanin prepropeptide	GAL	A	P	P	P	28.6	12.6	1.5	−1.5
207545_s_at	Hs.654609	Numb homolog (Drosophila)	NUMB	P	P	P	P	1.1	1.2	1.9	2.0
207742_s_at	Hs.586460	Nuclear receptor subfamily 6, group A, member 1	NR6A1	A	A	A	A	11.4	19.9	−2.2	−1.2
208275_x_at	Hs.458406	Undifferentiated embryonic cell transcription factor 1	UTF1	A	P	P	P	13.0	29.6	1.1	2.5
208286_x_at	Hs.632482	POU class 5 homeobox 1 POU class 5 homeobox 1B POU class 5 homeobox 1 pseudogene 3 POU class 5 homeobox 1 pseudogene 4	POU5F1 POU5F1B POU5F1P3 POU5F1P4	A	P	P	P	1925.3	2025.3	1.1	1.2
208337_s_at	Hs.33446	Nuclear receptor subfamily 5, group A, member 2	NR5A2	A	P	P	P	37.8	26.4	1.0	−1.4
208343_s_at	Hs.33446	Nuclear receptor subfamily 5, group A, member 2	NR5A2	A	P	P	P	153.3	39.3	1.4	−2.7
208378_x_at	Hs.37055	Fibroblast growth factor 5	FGF5	P	A	A	A	−9.8	−55.8	1.9	−3.0
208500_x_at	Hs.546573	Forkhead box D3	FOXD3	A	A	A	A	5.5	14.1	−7.9	−3.1
209073_s_at	Hs.654609	Numb homolog (Drosophila)	NUMB	P	P	P	P	−1.2	1.1	1.1	1.4
210002_at	Hs.514746	GATA binding protein 6	GATA6	P	A	A	A	−38.1	−4.8	−1.3	6.0
210174_at	Hs.33446	Nuclear receptor subfamily 5, group A, member 2	NR5A2	A	P	P	P	28.8	9.6	2.3	−1.3
210310_s_at	Hs.37055	Fibroblast growth factor 5	FGF5	P	A	A	A	−127.2	−102.7	−1.4	−1.1
210311_at	Hs.37055	Fibroblast growth factor 5	FGF5	P	A	M	A	−4.5	−6.8	1.6	1.0
210391_at	Hs.586460	Nuclear receptor subfamily 6, group A, member 1	NR6A1	A	A	A	A	1.5	4.1	−1.5	1.7
210392_x_at	Hs.586460	Nuclear receptor subfamily 6, group A, member 1	NR6A1	A	M	A	A	6.7	6.1	1.2	1.1
210560_at	Hs.184945	Gastrulation brain homeobox 2	GBX2	A	A	A	A	4.5	10.3	3.6	8.4
210761_s_at	Hs.86859	Growth factor receptor-bound protein 7	GRB7	A	P	P	P	1.6	3.2	−1.3	1.5
211000_s_at	Hs.532082	Interleukin 6 signal transducer (gp130, oncostatin M receptor)	IL6ST	P	A	A	A	−8.2	−7.5	1.3	1.5
211402_x_at	Hs.586460	Nuclear receptor subfamily 6, group A, member 1	NR6A1	A	A	A	A	13.6	10.7	−1.0	−1.3
211711_s_at	Hs.500466	Phosphatase and tensin homolog	PTEN	P	P	P	P	−1.8	−2.2	1.0	−1.2
212195_at	Hs.532082	Interleukin 6 signal transducer (gp130, oncostatin M receptor)	IL6ST	P	P	P	P	−17.9	−15.2	1.2	1.4
212196_at	Hs.532082	Interleukin 6 signal transducer (gp130, oncostatin M receptor)	IL6ST	P	P	P	P	−4.2	−3.7	1.1	1.3
212920_at	Hs.631513	RE1-silencing transcription factor	REST	P	P	P	P	1.5	2.4	−1.1	1.4
213721_at	Hs.518438	SRY (sex-determining region Y)-box 2	SOX2	A	P	P	P	72.0	53.6	1.1	−1.3
213722_at	Hs.518438	SRY (sex-determining region Y)-box 2	SOX2	A	A	A	A	9.6	2.9	1.4	−2.3
214022_s_at	Hs.458414	Interferon-induced transmembrane protein 1 (9-27)	IFITM1	P	P	P	P	5.7	6.1	1.7	1.8

Probe Set ID	UniGene ID	Gene Title	Symbol	Flag[a]				Fold Change Versus DMC54		Fold Change Versus KhES1	
				DMC54	DMC5403	DMC5413	KhES1	DMC5403	DMC5413	DMC5403	DMC5413
214178_s_at	Hs.518438	SRY (sex-determining region Y)-box 2	SOX2	A	A	A	A	4.3	3.3	1.4	1.1
214218_s_at	Hs.730656	X (inactive)-specific transcript (nonprotein coding)	XIST	P	P	P	P	−1.0	−60.2	80.1	1.4
214240_at	Hs.278959	Galanin prepropeptide	GAL	A	P	P	P	3871.9	2443.0	1.6	−1.0
217246_s_at	Hs.226483	Diaphanous homolog 2 (Drosophila)	DIAPH2	A	A	A	P	1.4	1.2	−1.1	−1.3
218048_at	Hs.720384	COMM domain containing 3	COMMD3	P	P	P	P	−5.1	−9.7	1.3	−1.4
218847_at	Hs.35354	Insulin-like growth factor 2 mRNA binding protein 2	IGF2BP2	P	P	P	P	2.2	2.8	1.1	1.5
219177_at	Hs.718510	BRX1, biogenesis of ribosomes, homolog (*S. cerevisiae*)	BRIX1	P	P	P	P	1.6	2.8	−1.1	1.6
219735_s_at	Hs.156471	Transcription factor CP2-like 1	TFCP2L1	A	P	P	P	3.5	2.7	1.2	−1.1
219823_at	Hs.86154	Lin-28 homolog (*C. elegans*)	LIN28	A	P	P	P	25980.2	23501.4	1.1	1.0
220053_at	Hs.86232	Growth differentiation factor 3	GDF3	A	P	P	P	15.8	22.7	−1.1	1.3
220184_at	Hs.635882	Nanog homeobox	NANOG	A	P	P	P	15134.8	13855.2	1.4	1.3
220668_s_at	Hs.643024	DNA (cytosine-5-)-methyltransferase 3β	DNMT3B	P	P	P	P	99.7	82.3	1.2	−1.1
221728_x_at	Hs.730656	X (inactive)-specific transcript (nonprotein coding)	XIST	P	P	A	A	−1.3	−88.8	1945.5	27.6
222176_at	Hs.500466	Phosphatase and tensin homolog	PTEN	A	A	A	A	−3.7	−7.5	−3.4	−6.9
223121_s_at	Hs.481022	Secreted frizzled-related protein 2	SFRP2	A	P	P	P	258.7	375.6	−1.1	1.3
223122_s_at	Hs.481022	Secreted frizzled-related protein 2	SFRP2	A	P	P	P	1264.8	14.76.7	−1.4	−1.2
223963_s_at	Hs.35354	Insulin-like growth factor 2 mRNA binding protein 2	IGF2BP2	P	M	P	A	1.3	1.4	−1.2	−1.1
224588_at	Hs.730656	X (inactive)-specific transcript (nonprotein coding)	XIST	P	P	A	A	−1.3	−176.7	355.0	2.7
224589_at	Hs.730656	X (inactive)-specific transcript (nonprotein coding)	XIST	P	P	A	A	−2.5	−187.9	7.8	−9.6
224590_at	Hs.730656	X (inactive)-specific transcript (nonprotein coding)	XIST	P	P	A	A	−5.7	−128.8	34.4	1.5
225363_at	Hs.500466	Phosphatase and tensin homolog	PTEN	P	P	P	P	−1.9	−3.0	1.1	−1.4
225571_at	Hs.133421	Leukemia inhibitory factor receptor α	LIFR	P	P	P	P	14.0	14.3	1.3	1.3
225575_at	Hs.133421	Leukemia inhibitory factor receptor α	LIFR	P	P	P	P	6.4	6.5	1.4	1.4
227642_at	Hs.156471	Transcription factor CP2-like 1	TFCP2L1	A	P	P	P	29.3	33.4	1.4	1.6
227671_at	Hs.730656	X (inactive)-specific transcript (nonprotein coding)	XIST	P	P	A	A	−1.0	−66.6	44.9	−1.4
227690_at	Hs.302352	γ-Aminobutyric acid (GABA) A receptor, β3	GABRB3	A	P	P	P	133.3	161.2	1.0	1.2
227771_at	Hs.133421	Leukemia inhibitory factor receptor α	LIFR	P	P	P	P	2.9	1.8	1.1	−1.5
227830_at	Hs.302352	γ-Aminobutyric acid (GABA) A receptor, β3	GABRB3	A	P	P	P	121.6	129.7	1.2	1.2
228038_at	Hs.518438	SRY (sex-determining region Y)-box 2	SOX2	A	P	P	P	8739.3	7576.9	1.2	1.1
229282_at	Hs.514746	GATA binding protein 6	GATA6	M	M	P	A	1.7	1.6	3.1	3.0
229341_at	Hs.156471	Transcription factor CP2-like 1	TFCP2L1	A	A	A	A	1.2	2.9	−3.9	−1.6

(*continued*)

Table 3. Gene Expression Data of the Probe Sets in the Affymetrix Human Genome U133 Plus 2.0 Array for the Characterization of Undifferentiated Stem Cells (*Continued*)

				Flag[a]				Fold Change Versus DMC54		Fold Change Versus KhES1	
Probe Set ID	UniGene ID	Gene Title	Symbol	DMC54	DMC5403	DMC5413	KhES1	DMC5403	DMC5413	DMC5403	DMC5413
229724_at	Hs.302352	γ-Aminobutyric acid (GABA) A receptor, β3	GABRB3	A	P	P	P	51.7	53.0	1.2	1.3
230462_at	Hs.654609	Numb homolog (Drosophila)	NUMB	P	P	P	P	2.1	1.6	−1.4	−1.9
230916_at	Hs.370414	Nodal homolog (mouse)	NODAL	A	P	P	P	26.2	27.7	1.0	1.1
231798_at	Hs.248201	Noggin	NOG	P	P	P	P	−17.0	−13.5	1.2	1.5
233254_x_at	Hs.500466	Phosphatase and tensin homolog	PTEN	A	A	A	A	1.1	−1.6	−1.1	−2.0
233314_at	Hs.500466	Phosphatase and tensin homolog	PTEN	A	P	A	P	17.2	2.4	1.0	−7.2
233317_at	Hs.114286	CD9 molecule	CD9	A	A	A	A	8.2	1.9	1.4	−3.0
233322_at	Hs.114286	CD9 molecule	CD9	A	A	A	A	2.1	1.9	5.7	5.0
234474_x_at	Hs.532082	Interleukin 6 signal transducer (gp130, oncostatin M receptor)	IL6ST	A	A	A	A	−9.9	−15.9	−1.8	−2.9
234967_at	Hs.532082	Interleukin 6 signal transducer (gp130, oncostatin M receptor)	IL6ST	A	A	A	A	−2.8	−3.0	−4.4	−4.8
235446_at	Hs.724376	X (inactive)-specific transcript (nonprotein coding)	XIST	A	A	A	A	1.5	−1.1	1.2	−1.4
236930_at	Hs.654609	Numb homolog (Drosophila)	NUMB	A	P	P	P	2.3	2.1	−1.6	−1.7
237896_at	Hs.370414	Nodal homolog (mouse)	NODAL	A	P	P	P	6.3	5.6	1.1	−1.0
241609_at	Hs.546573	Forkhead box D3	FOXD3	A	A	A	A	2.9	7.7	2.0	5.3
241612_at	Hs.546573	Forkhead box D3	FOXD3	A	P	P	P	758.4	868.1	1.0	1.2
242622_x_at	Hs.500466	Phosphatase and tensin homolog	PTEN	A	A	A	A	1.2	−1.1	−2.6	−3.6
243161_x_at	Hs.335787	Zinc finger protein 42 homolog (mouse)	ZFP42	A	P	P	P	8492.4	8389.2	−1.3	−1.3
243712_at	Hs.730656	X (inactive)-specific transcript (nonprotein coding)	XIST	A	A	A	A	1.3	1.9	−1.8	−1.2
244163_at	Hs.252451	Sema domain, immunoglobulin domain (Ig), short basic domain, secreted, (semaphorin) 3A	SEMA3A	P	P	P	P	1.2	−1.2	1.7	1.2
244849_at	Hs.252451	Sema domain, immunoglobulin domain (Ig), short basic domain, secreted, (semaphorin) 3A	SEMA3A	P	P	A	P	1.8	−1.4	1.3	−1.9

[a]Flag indicates whether a transcript is present (P), marginal (M), or absent (A), as assigned by the Detection Algorithm.

or fewer factors, that is, c-MYC is not required (30). Although we tried several times to reprogram the DMCs using OSK, we could not generate hiPSCs (unpublished results). The lower endogenous expression of MYCL1 in the DMCs compared with DFBs might explain the reduced efficiency of DMC reprogramming when c-MYC is omitted.

We also evaluated the expression of the GLIS1 homologs GLIS2 and GLIS3 in several cell lines and tissues (Fig. 8). GLIS2 and GLIS3 were hardly expressed in pluripotent stem cells (hESCs and hiPSCs), placenta, or testis (Fig. 8). In contrast, placenta-derived cells (AECs, AMCs, DMCs), BM-MSCs, and DFBs expressed GLIS2 and GLIS3; in particular, DFBs highly expressed both GLIS1 homologs (Fig. 8). Although the significance of GLIS2 and GLIS3 in generating hiPSCs is not yet clear, these differences in GLI-related Krüppel-like zinc finger genes might result in different efficiencies of hiPSC generation from various cell sources. Another factor, Zscan4, was previously shown to facilitate the reprogramming of MEFs (12). Unlike in MEFs, we detected an increase in the intrinsic expression of ZSCAN4 in human DMCs and DFBs when the reprogramming factors were overexpressed; however, ZSCAN4's contribution to iPSC generation has yet to be elucidated. Zscan4 was shown to be required only for the first few days of iPSC formation and to mediate the activation of genes detected only in preimplantation embryos (1-cell to blastocyst) (12). Besides

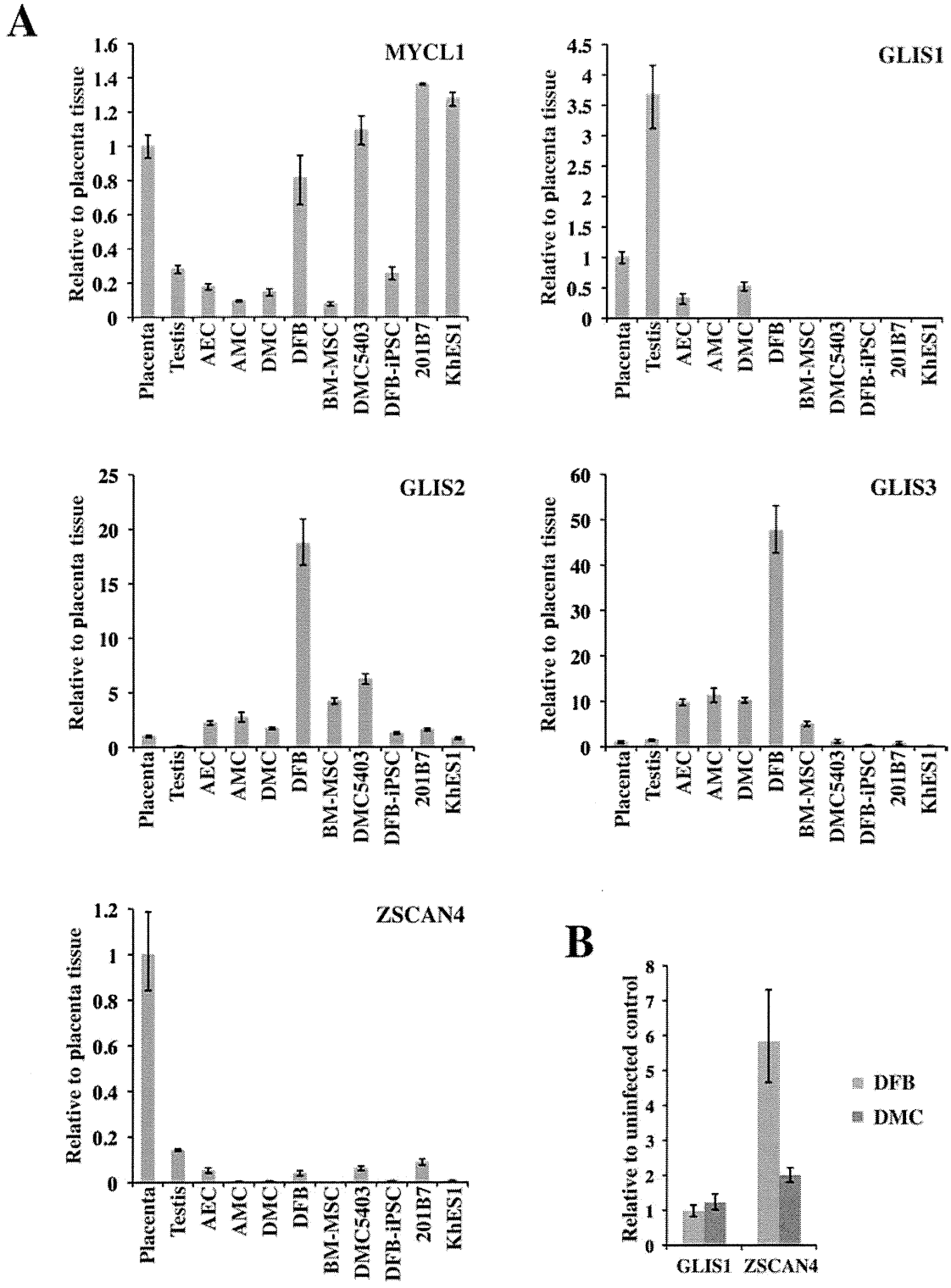

Figure 8. Transcriptional expression of novel factors for efficient reprogramming. (A) Endogenous transcriptional expression of MYCL1 (top left), GLIS1 (top right), GLIS2 (middle left), GLIS3 (middle right), and ZSCAN4 (bottom left). GAPDH was used as the internal control gene, and data are presented relative to the values from placenta tissue and as the mean ± SD (n=3). (B) Expression of GLIS1 and ZSCAN4 3 days after the transduction of reprogramming factor genes. Results are shown in comparison to individual uninfected control cells. See Table 1 for gene definitions.

GLIS1 and ZSCAN4, other preimplantation-specific genes that are expressed in blastomeres and have reprogramming activity in nuclear transplantation (5) should be considered for improving the generation of iPSCs.

Molecular Characteristics of DMC-hiPSCs

The global expression profile of DMC-iPSC clones, which retained a hESC-like morphology after several passages, verified that there was a strong similarity between DMC-hiPSCs and KhES1 ($p > 0.98$) (Fig. 7A). Despite the similarities, one of the genes for characterizing undifferentiated ES cells (2), XIST, was highly expressed in one of the DMC-iPSC clones (DMC5403), that is, at more than 10 times the level in female hESCs (KhES1), and at the same level as in the parental DMCs. In female cells, one of the two X-chromosomes is transcriptionally silenced through a process called X-chromosome inactivation (XCI); this process depends on the large noncoding RNA XIST (45). In the mouse system, the key pluripotency factors Nanog, Oct3/4, and Sox2 bind within Xist's intron 1 and cooperate to repress the Xist transcript in undifferentiated embryonic stem (ES) cells; therefore, both X-chromosomes remain active (Xa) (32). In the process of reprogramming female somatic cells to miPSCs, the inactivated X-chromosome (Xi) is reactivated in concert with the activation of pluripotency factors (25,40). On the other hand, the X-chromosomes of female hESCs have a variable epigenetic status (2,39), and many hESC lines display XCI in the undifferentiated state. Studies of the epigenetic state of the X-chromosomes in hiPSCs have led to two conflicting conclusions. One study showed that a hiPSC clone, unlike miPSCs, was reprogrammed without undergoing X-reactivation and maintained the XCI of the mother fibroblast cell (44). Another study showed that complete X-reactivation was achieved in some hiPSC lines and that subsequent X-inactivation occurred during differentiation (26).

We briefly examined the epigenetic state by assessing the XIST expression and performing MSP analysis of the XIST promoter region. In agreement with the expectation that XIST would be silenced on Xa and actively expressed from Xi, the results indicated that Xi/Xa was present in the parental female cells and in the early phase of one DMC-hiPSC clone (DMC5403 at passage 5). In contrast, Xa/Xa was present in the other DMC-hiPSC clone (DMC5413) and in DFB-hiPSCs (Fig. 7B). DMC5403 cells from multiply passaged cultures did not express the XIST gene, although the XIST promoter region in half of the chromosomes remained unmethylated. The silencing of XIST expression in the presence of an inactive X is often observed in both undifferentiated and differentiated cell states (39,44). Overall, regardless of the epigenetic state of the X-chromosome, the DMC-iPSC clones exhibited genome-wide expression profiles similar to those of hESCs and formed differentiated tissues containing all three germ layers in vitro and in vivo (early passage, Figs. 5–7) (late passage, data not shown). Thus, not just the X-chromosome but the overall epigenetic state of iPSCs is an important quality and safety concern in clinical applications of hiPSCs and remains to be fully addressed.

DMC-hiPSCs May Be Useful as Allogeneic hiPSCs in Regenerative Medicine

Extraembryonic tissues such as the umbilical cord and placenta have been proposed as attractive human cell sources for use in regenerative medicine. In addition, human amnion-derived cells, which are of fetal origin, were reported as a promising cell source for efficient hiPSC generation (4,29,48). In this study, we used DMCs isolated from the decidua membrane, which is a maternal portion of the placenta (18). DMCs exhibit a typical fibroblast-like morphology and have a high proliferative potential for over 30 population doublings, which is better than that of BM-MSCs (18). They strongly express the mesenchymal cell marker vimentin, but not cytokeratin 19 or HLA-G, and FCM analysis shows a resemblance between DMCs and BM-MSCs. In vitro, the DMCs showed good differentiation into chondrocytes and moderate differentiation into adipocytes, but scant evidence of osteogenesis, compared with BM-MSCs. These findings indicated that DMCs are mesenchymal cells of purely maternal origin and unique cells that have MSC-like properties but differ from BM-MSCs. It was previously reported that mesenchymal cells derived from the human term decidua are multipotent, and these decidua-derived mesenchymal cells were suggested to be useful for regenerative medicine (11,13,23). However, in the mouse system, MSCs purified from adult tissue are useful for producing high-quality iPSCs (33). In addition, iPSCs have been generated efficiently from various somatic stem cells, including MSCs (4,33,35) and neural stem cells (6,19). In this context, the generation of iPSCs from immature somatic stem cells is an important option that needs to be thoroughly examined.

Here, we showed that DMCs can be efficiently reprogrammed into pluripotent stem cells. Although DMCs are not superior to BM-MSCs in their multipotency and might have some risk of genomic abnormalities accumulated during aging, their greater proliferative ability means that their cultivation might require less maintenance, and their derivation from the maternal portion of the human fetal adnexal tissues, which are otherwise discarded, would resolve many ethical concerns associated with the use of embryonic stem cells. The high success rate of DMC isolation from tissues stored more than 24 h indicates that it may be feasible to develop a system for collecting and banking fetal adnexal tissues; such a bank would provide

tissues of wide HLA variation to multiple and even remote hospitals (18). We also previously reported that the pericellular matrix prepared from DMCs (PCM-DM) is as potent a substrate for the growth and pluripotency of hESCs as Matrigel (28). Furthermore, we have confirmed that hiPSCs can be generated on PCM-DM by a retroviral gene transduction procedure (Fukusumi et al., submitted).

To be sure, many concerns about the feasibility and potential risks of cell-based therapies using iPSCs have been recognized, and many scientific and technical issues remain to be elucidated before iPSC technology can be applied to regenerative medicine. Since patient safety is the foremost consideration, extensive exploration and testing of iPSCs will be required before this technology can be considered for clinical use.

Taken together, these findings indicate that DMCs have several advantages for clinical use and that the generation of hiPSCs from DMCs might enable the establishment of hiPSC-banking systems. Such systems could increase the availability of allogeneic hiPSCs that have broad HLA variations and thus increase the feasibility of their use in clinical applications.

ACKNOWLEDGMENTS: We thank Dr. Chiaki Ban (Department of Obstetrics and Gynecology Osaka National Hospital) and Ms. Chika Teramoto and Ms. Ai Takada (Osaka National Hospital) for support in collecting the human placenta tissues. We also thank Mr. Kenji Kawai and Ms. Miyuki Kuromuma (CIEA) for support in the teratoma formation assay. This study was supported by the Project for the Realization of Regenerative Medicine, the Ministry of Education, Culture, Sports, Science and Technology (MEXT) of Japan, the Cooperative Link of Unique Science and Technology for Economy Revitalization (CLUSTER) project from MEXT, Japan, and the Research on New Drug Development, Health and Labour Sciences Research Grants, the Ministry of Health, Labour and Welfare (MHLW) of Japan. The authors declare no conflicts of interest.

REFERENCES

1. Aasen, T.; Raya, A.; Barrero, M. J.; Garreta, E.; Consiglio, A.; Gonzalez, F.; Vassena, R.; Bilic, J.; Pekarik, V.; Tiscornia, G.; Edel, M.; Boue, S.; Izpisua Belmonte, J. C. Efficient and rapid generation of induced pluripotent stem cells from human keratinocytes. Nat. Biotechnol. 26(11):1276–1284; 2008.
2. Adewumi, O.; Aflatoonian, B.; Ahrlund-Richter, L.; Amit, M.; Andrews, P. W.; Beighton, G.; Bello, P. A.; Benvenisty, N.; Berry, L. S.; Bevan, S.; Blum, B.; Brooking, J.; Chen, K. G.; Choo, A. B. H.; Churchill, G. A.; Corbel, M.; Damjanov, I.; Draper, J. S.; Dvorak, P.; Emanuelsson, K.; Fleck, R. A.; Ford, A.; Gertow, K.; Gertsenstein, M.; Gokhale, P. J.; Hamilton, R. S.; Hampl, A.; Healy, L. E.; Hovatta, O.; Hyllner, J.; Imreh, M. P.; Itskovitz-Eldor, J.; Jackson, J.; Johnson, J. L.; Jones, M.; Kee, K.; King, B. L.; Knowles, B. B.; Lako, M.; Lebrin, F.; Mallon, B. S.; Manning, D.; Mayshar, Y.; McKay, R. D. G.; Michalska, A. E.; Mikkola, M.; Mileikovsky, M.; Minger, S. L.; Moore, H. D.; Mummery, C. L.; Nagy, A.; Nakatsuji, N.; O'Brien, C. M.; Oh, S. K. W.; Olsson, C.; Otonkoski, T.; Park, K.-Y.; Passier, R.; Patel, H.; Patel, M.; Pedersen, R.; Pera, M. F.; Piekarczyk, M. S.; Pera, R. A. R.; Reubinoff, B. E.; Robins, A. J.; Rossant, J.; Rugg-Gunn, P.; Schulz, T. C.; Semb, H.; Sherrer, E. S.; Siemen, H.; Stacey, G. N.; Stojkovic, M.; Suemori, H.; Szatkiewicz, J.; Turetsky, T.; Tuuri, T.; van den Brink, S.; Vintersten, K.; Vuoristo, S.; Ward, D.; Weaver, T. A.; Young, L. A.; Zhang, W. Characterization of human embryonic stem cell lines by the International Stem Cell Initiative. Nat. Biotechnol. 25(7):803–816; 2007.
3. Barlow, S.; Brooke, G.; Chatterjee, K.; Price, G.; Pelekanos, R.; Rossetti, T.; Doody, M.; Venter, D.; Pain, S.; Gilshenan, K.; Atkinson, K. Comparison of human placenta- and bone marrow-derived multipotent mesenchymal stem cells. Stem Cells Dev. 17:1095–1107; 2008.
4. Cai, J.; Li, W.; Su, H.; Qin, D.; Yang, J.; Zhu, F.; Xu, J.; He, W.; Guo, X.; Labuda, K.; Peterbauer, A.; Wolbank, S.; Zhong, M.; Li, Z.; Wu, W.; So, K. F.; Redl, H.; Zeng, L.; Esteban, M. A.; Pei, D. Generation of human induced pluripotent stem cells from umbilical cord matrix and amniotic membrane mesenchymal cells. J. Biol. Chem. 285:11227–11234; 2010.
5. Egli, D.; Sandler, V. M.; Shinohara, M. L.; Cantor, H.; Eggan, K. Reprogramming after chromosome transfer into mouse blastomeres. Curr. Biol. 19:1403–1409; 2009.
6. Eminli, S.; Utikal, J.; Arnold, K.; Jaenisch, R.; Hochedlinger, K. Reprogramming of neural progenitor cells into induced pluripotent stem cells in the absence of exogenous Sox2 expression. Stem Cells 26:2467–2474; 2008.
7. Falco, G.; Lee, S. L.; Stanghellini, I.; Bassey, U. C.; Hamatani, T.; Ko, M. S. Zscan4: A novel gene expressed exclusively in late 2-cell embryos and embryonic stem cells. Dev. Biol. 307:539–550; 2007.
8. Fukuchi, Y.; Nakajima, H.; Sugiyama, D.; Hirose, I.; Kitamura, T.; Tsuji, K. Human placenta-derived cells have mesenchymal stem/progenitor cell potential. Stem Cells 22:649–658; 2004.
9. Haase, A.; Olmer, R.; Schwanke, K.; Wunderlich, S.; Merkert, S.; Hess, C.; Zweigerdt, R.; Gruh, I.; Meyer, J.; Wagner, S.; Maier, L. S.; Han, D. W.; Glage, S.; Miller, K.; Fischer, P.; Scholer, H. R.; Martin, U. Generation of induced pluripotent stem cells from human cord blood. Cell Stem Cell 5:434–441; 2009.
10. Hanna, J.; Markoulaki, S.; Schorderet, P.; Carey, B. W.; Beard, C.; Wernig, M.; Creyghton, M. P.; Steine, E. J.; Cassady, J. P.; Foreman, R.; Lengner, C. J.; Dausman, J. A.; Jaenisch, R. Direct reprogramming of terminally differentiated mature B lymphocytes to pluripotency. Cell 133:250–264; 2008.
11. Hayati, A. R.; Nur Fariha, M. M.; Tan, G. C.; Tan, A. E.; Chua, K. Potential of human decidua stem cells for angiogenesis and neurogenesis. Arch. Med. Res. 42:291–300; 2011.
12. Hirata, T.; Amano, T.; Nakatake, Y.; Amano, M.; Piao, Y.; Hoang, H. G.; Ko, M. S. Zscan4 transiently reactivates early embryonic genes during the generation of induced pluripotent stem cells. Sci. Rep. 2:208; 2012.
13. Huang, Y. C.; Yang, Z. M.; Chen, X. H.; Tan, M. Y.; Wang, J.; Li, X. Q.; Xie, H. Q.; Deng, L. Isolation of mesenchymal stem cells from human placental decidua basalis and resistance to hypoxia and serum deprivation. Stem Cell Rev. 5:247–255; 2009.
14. Igura, K.; Zhang, X.; Takahashi, K.; Mitsuru, A.; Yamaguchi, S.; Takashi, T. A. Isolation and characterization of mesenchymal progenitor cells from chorionic villi of human placenta. Cytotherapy 6:543–553; 2004.

15. In 't Anker, P. S.; Scherjon, S. A.; Kleijburg-van der Keur, C.; de Groot-Swings, G. M.; Claas, F. H.; Fibbe, W. E.; Kanhai, H. H. Isolation of mesenchymal stem cells of fetal or maternal origin from human placenta. Stem Cells 22:1338–1345; 2004.
16. Ito, M.; Hiramatsu, H.; Kobayashi, K.; Suzue, K.; Kawahata, M.; Hioki, K.; Ueyama, Y.; Koyanagi, Y.; Sugamura, K.; Tsuji, K.; Heike, T.; Nakahata, T. NOD/SCID/gamma(c) (null) mouse: An excellent recipient mouse model for engraftment of human cells. Blood 100:3175–3182; 2002.
17. Izumi, M.; Pazin, B. J.; Minervini, C. F.; Gerlach, J.; Ross, M. A.; Stolz, D. B.; Turner, M. E.; Thompson, R. L.; Miki, T. Quantitative comparison of stem cell marker-positive cells in fetal and term human amnion. J. Reprod. Immunol. 81:39–43; 2009.
18. Kanematsu, D.; Shofuda, T.; Yamamoto, A.; Ban, C.; Ueda, T.; Yamasaki, M.; Kanemura, Y. Isolation and cellular properties of mesenchymal cells derived from the decidua of human term placenta. Differentiation 82:77–88; 2011.
19. Kim, J. B.; Sebastiano, V.; Wu, G.; Arauzo-Bravo, M. J.; Sasse, P.; Gentile, L.; Ko, K.; Ruau, D.; Ehrich, M.; van den Boom, D.; Meyer, J.; Hubner, K.; Bernemann, C.; Ortmeier, C.; Zenke, M.; Fleischmann, B. K.; Zaehres, H.; Scholer, H. R. Oct4-induced pluripotency in adult neural stem cells. Cell 136:411–419; 2009.
20. Livak, K. J.; Schmittgen, T. D. Analysis of relative gene expression data using real-time quantitative PCR and the 2(-Delta Delta C(T)) Method. Methods 25:402–408; 2001.
21. Loh, Y. H.; Agarwal, S.; Park, I. H.; Urbach, A.; Huo, H.; Heffner, G. C.; Kim, K.; Miller, J. D.; Ng, K.; Daley, G. Q. Generation of induced pluripotent stem cells from human blood. Blood 113:5476–5479; 2009.
22. Lowry, W. E.; Richter, L.; Yachechko, R.; Pyle, A. D.; Tchieu, J.; Sridharan, R.; Clark, A. T.; Plath, K. Generation of human induced pluripotent stem cells from dermal fibroblasts. Proc. Natl. Acad. Sci. USA 105:2883–2888; 2008.
23. Macias, M. I.; Grande, J.; Moreno, A.; Dominguez, I.; Bornstein, R.; Flores, A. I. Isolation and characterization of true mesenchymal stem cells derived from human term decidua capable of multilineage differentiation into all 3 embryonic layers. Am. J. Obstet. Gynecol. 203:e495; 2010.
24. Maekawa, M.; Yamaguchi, K.; Nakamura, T.; Shibukawa, R.; Kodanaka, I.; Ichisaka, T.; Kawamura, Y.; Mochizuki, H.; Goshima, N.; Yamanaka, S. Direct reprogramming of somatic cells is promoted by maternal transcription factor Glis1. Nature 474:225–229; 2011.
25. Maherali, N.; Sridharan, R.; Xie, W.; Utikal, J.; Eminli, S.; Arnold, K.; Stadtfeld, M.; Yachechko, R.; Tchieu, J.; Jaenisch, R.; Plath, K.; Hochedlinger, K. Directly reprogrammed fibroblasts show global epigenetic remodeling and widespread tissue contribution. Cell Stem Cell 1:55–70; 2007.
26. Marchetto, M. C. N.; Carromeu, C.; Acab, A.; Yu, D.; Yeo, G. W.; Mu, Y.; Chen, G.; Gage, F. H.; Muotri, A. R. A Model for neural development and treatment of rett syndrome using human induced pluripotent stem cells. Cell 143:527–539; 2010.
27. Meissner, A.; Wernig, M.; Jaenisch, R. Direct reprogramming of genetically unmodified fibroblasts into pluripotent stem cells. Nat. Biotechnol. 25:1177–1181; 2007.
28. Nagase, T.; Ueno, M.; Matsumura, M.; Muguruma, K.; Ohgushi, M.; Kondo, N.; Kanematsu, D.; Kanemura, Y.; Sasai, Y. Pericellular matrix of decidua-derived mesenchymal cells: A potent human-derived substrate for the maintenance culture of human ES cells. Dev. Dyn. 238: 1118–1130; 2009.
29. Nagata, S.; Toyoda, M.; Yamaguchi, S.; Hirano, K.; Makino, H.; Nishino, K.; Miyagawa, Y.; Okita, H.; Kiyokawa, N.; Nakagawa, M.; Yamanaka, S.; Akutsu, H.; Umezawa, A.; Tada, T. Efficient reprogramming of human and mouse primary extraembryonic cells to pluripotent stem cells. Genes Cells 14:1395–1404; 2009.
30. Nakagawa, M.; Koyanagi, M.; Tanabe, K.; Takahashi, K.; Ichisaka, T.; Aoi, T.; Okita, K.; Mochiduki, Y.; Takizawa, N.; Yamanaka, S. Generation of induced pluripotent stem cells without Myc from mouse and human fibroblasts. Nat. Biotechnol. 26:101–106; 2008.
31. Nakagawa, M.; Takizawa, N.; Narita, M.; Ichisaka, T.; Yamanaka, S. Promotion of direct reprogramming by transformation-deficient Myc. Proc. Natl. Acad. Sci. USA 107:14152–14157; 2010.
32. Navarro, P.; Chambers, I.; Karwacki-Neisius, V.; Chureau, C.; Morey, C.; Rougeulle, C.; Avner, P. Molecular coupling of xist regulation and pluripotency. Science 321:1693–1695; 2008.
33. Niibe, K.; Kawamura, Y.; Araki, D.; Morikawa, S.; Miura, K.; Suzuki, S.; Shimmura, S.; Sunabori, T.; Mabuchi, Y.; Nagai, Y.; Nakagawa, T.; Okano, H.; Matsuzaki, Y. Purified mesenchymal stem cells are an efficient source for iPS cell induction. PLoS One 6:e17610; 2011.
34. Nori, S.; Okada, Y.; Yasuda, A.; Tsuji, O.; Takahashi, Y.; Kobayashi, Y.; Fujiyoshi, K.; Koike, M.; Uchiyama, Y.; Ikeda, E.; Toyama, Y.; Yamanaka, S.; Nakamura, M.; Okano, H. Grafted human-induced pluripotent stem cell-derived neurospheres promote motor functional recovery after spinal cord injury in mice. Proc. Nat. Acad. Sci. USA 108:16825–16830; 2011.
35. Oda, Y.; Yoshimura, Y.; Ohnishi, H.; Tadokoro, M.; Katsube, Y.; Sasao, M.; Kubo, Y.; Hattori, K.; Saito, S.; Horimoto, K.; Yuba, S.; Ohgushi, H. Induction of pluripotent stem cells from human third molar mesenchymal stromal cells. J. Biol. Chem. 285:29270–29278; 2010.
36. Okita, K.; Matsumura, Y.; Sato, Y.; Okada, A.; Morizane, A.; Okamoto, S.; Hong, H.; Nakagawa, M.; Tanabe, K.; Tezuka, K.-i.; Shibata, T.; Kunisada, T.; Takahashi, M.; Takahashi, J.; Saji, H.; Yamanaka, S. A more efficient method to generate integration-free human iPS cells. Nat. Methods 8:409–412; 2011.
37. Park, I. H.; Zhao, R.; West, J. A.; Yabuuchi, A.; Huo, H.; Ince, T. A.; Lerou, P. H.; Lensch, M. W.; Daley, G. Q. Reprogramming of human somatic cells to pluripotency with defined factors. Nature 451:141–146; 2008.
38. Silva, J.; Nichols, J.; Theunissen, T. W.; Guo, G.; van Oosten, A. L.; Barrandon, O.; Wray, J.; Yamanaka, S.; Chambers, I.; Smith, A. Nanog is the gateway to the pluripotent ground state. Cell 138:722–737; 2009.
39. Silva, S. S.; Rowntree, R. K.; Mekhoubad, S.; Lee, J. T. X-chromosome inactivation and epigenetic fluidity in human embryonic stem cells. Proc. Nat. Acad. Sci. USA 105:4820–4825; 2008.
40. Stadtfeld, M.; Maherali, N.; Breault, D. T.; Hochedlinger, K. Defining molecular cornerstones during fibroblast to iPS cell reprogramming in mouse. Cell Stem Cell 2:230–240; 2008.

41. Suemori, H.; Yasuchika, K.; Hasegawa, K.; Fujioka, T.; Tsuneyoshi, N.; Nakatsuji, N. Efficient establishment of human embryonic stem cell lines and long-term maintenance with stable karyotype by enzymatic bulk passage. Biochem. Biophys. Res. Commun. 345:926–932; 2006.
42. Takahashi, K.; Tanabe, K.; Ohnuki, M.; Narita, M.; Ichisaka, T.; Tomoda, K.; Yamanaka, S. Induction of pluripotent stem cells from adult human fibroblasts by defined factors. Cell 131:861–872; 2007.
43. Takahashi, K.; Yamanaka, S. Induction of pluripotent stem cells from mouse embryonic and adult fibroblast cultures by defined factors. Cell 126:663–676; 2006.
44. Tchieu, J.; Kuoy, E.; Chin, M. H.; Trinh, H.; Patterson, M.; Sherman, S. P.; Aimiuwu, O.; Lindgren, A.; Hakimian, S.; Zack, J. A.; Clark, A. T.; Pyle, A. D.; Lowry, W. E.; Plath, K. Female human iPSCs retain an inactive X chromosome. Cell Stem Cell 7:329–342; 2010.
45. Wutz, A.; Jaenisch, R. A shift from reversible to irreversible X inactivation is triggered during ES cell differentiation. Mol. Cell 5:695–705; 2000.
46. Yen, B. L.; Huang, H. I.; Chien, C. C.; Jui, H. Y.; Ko, B. S.; Yao, M.; Shun, C. T.; Yen, M. L.; Lee, M. C.; Chen, Y. C. Isolation of multipotent cells from human term placenta. Stem Cells 23:3–9; 2005.
47. Yu, J.; Vodyanik, M. A.; Smuga-Otto, K.; Antosiewicz-Bourget, J.; Frane, J. L.; Tian, S.; Nie, J.; Jonsdottir, G. A.; Ruotti, V.; Stewart, R.; Slukvin, I. I.; Thomson, J. A. Induced pluripotent stem cell lines derived from human somatic cells. Science 318:1917–1920; 2007.
48. Zhao, H. X.; Li, Y.; Jin, H. F.; Xie, L.; Liu, C.; Jiang, F.; Luo, Y. N.; Yin, G. W.; Wang, J.; Li, L. S.; Yao, Y. Q.; Wang, X. H. Rapid and efficient reprogramming of human amnion-derived cells into pluripotency by three factors OCT4/SOX2/NANOG. Differentiation 80:123–129; 2010.

Research Article

EASL EUROPEAN ASSOCIATION FOR THE STUDY OF THE LIVER | JOURNAL OF HEPATOLOGY

Generation of metabolically functioning hepatocytes from human pluripotent stem cells by FOXA2 and HNF1α transduction

Kazuo Takayama[1,2], Mitsuru Inamura[1,2], Kenji Kawabata[2,3], Michiko Sugawara[4], Kiyomi Kikuchi[4], Maiko Higuchi[2], Yasuhito Nagamoto[1,2], Hitoshi Watanabe[1,2], Katsuhisa Tashiro[2], Fuminori Sakurai[1], Takao Hayakawa[5,6], Miho Kusuda Furue[7,8], Hiroyuki Mizuguchi[1,2,9,*]

[1]*Laboratory of Biochemistry and Molecular Biology, Graduate School of Pharmaceutical Sciences, Osaka University, Osaka 565-0871, Japan;* [2]*Laboratory of Stem Cell Regulation, National Institute of Biomedical Innovation, Osaka 567-0085, Japan;* [3]*Laboratory of Biomedical Innovation, Graduate School of Pharmaceutical Sciences, Osaka University, Osaka 565-0871, Japan;* [4]*Tsukuba Laboratories, Eisai Co., Ltd., Ibaraki 300-2635, Japan;* [5]*Pharmaceutics and Medical Devices Agency, Tokyo 100-0013, Japan;* [6]*Pharmaceutical Research and Technology Institute, Kinki University, Osaka 577-8502, Japan;* [7]*Laboratory of Cell Cultures, Department of Disease Bioresources Research, National Institute of Biomedical Innovation, Osaka 567-0085, Japan;* [8]*Laboratory of Cell Processing, Institute for Frontier Medical Sciences, Kyoto University, Kyoto 606-8507, Japan;* [9]*The Center for Advanced Medical Engineering and Informatics, Osaka University, Osaka 565-0871, Japan*

Background & Aims: Hepatocyte-like cells differentiated from human embryonic stem cells (hESCs) and induced pluripotent stem cells (hiPSCs) can be utilized as a tool for screening for hepatotoxicity in the early phase of pharmaceutical development. We have recently reported that hepatic differentiation is promoted by sequential transduction of SOX17, HEX, and HNF4α into hESC- or hiPSC-derived cells, but further maturation of hepatocyte-like cells is required for widespread use of drug screening.
Methods: To screen for hepatic differentiation-promoting factors, we tested the seven candidate genes related to liver development.
Results: The combination of two transcription factors, FOXA2 and HNF1α, promoted efficient hepatic differentiation from hESCs and hiPSCs. The expression profile of hepatocyte-related genes (such as genes encoding cytochrome P450 enzymes, conjugating enzymes, hepatic transporters, and hepatic nuclear receptors) achieved with FOXA2 and HNF1α transduction was comparable to that obtained in primary human hepatocytes. The hepatocyte-like cells generated by FOXA2 and HNF1α transduction exerted various hepatocyte functions including albumin and urea secretion, and the uptake of indocyanine green and low density lipoprotein. Moreover, these cells had the capacity to metabolize all nine tested drugs and were successfully employed to evaluate drug-induced cytotoxicity.
Conclusions: Our method employing the transduction of FOXA2 and HNF1α represents a useful tool for the efficient generation of metabolically functional hepatocytes from hESCs and hiPSCs, and the screening of drug-induced cytotoxicity.

Keywords: FOXA2; HNF1α; Hepatocytes; Adenovirus; Drug screening; Drug metabolism; hESCs; hiPSCs.
Received 14 November 2011; received in revised form 31 March 2012; accepted 4 April 2012; available online 29 May 2012
* Corresponding author. Address: Laboratory of Biochemistry and Molecular Biology, Graduate School of Pharmaceutical Sciences, Osaka University, 1-6 Yamadaoka, Suita, Osaka 565-0871, Japan. Tel.: +81 6 6879 8185; fax: +81 6 6879 8186.
E-mail address: mizuguch@phs.osaka-u.ac.jp (H. Mizuguchi).

Introduction

Hepatocyte-like cells differentiated from human embryonic stem cells (hESCs) [1] or human induced pluripotent stem cells (hiPSCs) [2] have more advantages than primary human hepatocytes (PHs) for drug screening. While application of PHs in drug screening has been hindered by lack of cellular growth, loss of function, and de-differentiation *in vitro* [3], hESC- or hiPSC-derived hepatocyte-like cells (hESC-hepa or hiPSC-hepa, respectively) have potential to solve these problems.

Hepatic differentiation from hESCs and hiPSCs can be divided into four stages: definitive endoderm (DE) differentiation, hepatic commitment, hepatic expansion, and hepatic maturation. Various growth factors are required to mimic liver development [4] and to promote hepatic differentiation. Previously, we showed that transduction of transcription factors in addition to treatment with optimal growth factors was effective to enhance hepatic differentiation [5–7]. An almost homogeneous hepatocyte population was obtained by sequential transduction of SOX17, HEX, and HNF4α into hESC- or hiPSCs-derived cells [7]. However, further maturation of the hESC-hepa and hiPSC-hepa is required for widespread use of drug screening because the drug metabolism capacity of these cells was not sufficient.

In some previous reports, hESC-hepa and hiPSC-hepa have been characterized for their hepatocyte functions in numerous ways, including functional assessment such as glycogen storage and low density lipoprotein (LDL) uptake [7]. To make a more precise judgment as to whether hESC-hepa and hiPSC-hepa can be applied to drug screening, it is more important to assess cytochrome P450 (CYP) induction potency and drug metabolism capacity rather than general hepatocyte function. Although Duan *et al.* have examined the drug metabolism capacity of hESC-hepa, drug metabolites were measured at 24 or 48 h [8]. To precisely

estimate the drug metabolism capacity, the amount of metabolites must be measured during the time when production of metabolites is linearly detected (generally before 24 h). To the best of our knowledge, there have been few reports that have examined various drugs metabolism capacity of hESC-hepa and hiPSC-hepa in detail.

In the present study, seven candidate genes (*FOXA2*, *HEX*, *HNF1α*, *HNF1β*, *HNF4α*, *HNF6*, and *SOX17*) were transduced into each stage of hepatic differentiation from hESCs by using an adenovirus (Ad) vector to screen for hepatic differentiation-promoting factors. Then, hepatocyte-related gene expression profiles and hepatocyte functions in hESC-hepa and hiPSC-hepa generated by the optimized protocol, were examined to investigate whether these cells have PHs characteristics. We used nine drugs, which are metabolized by various CYP enzymes and UDP-glucuronosyltransferases (UGTs), to determine whether the hESC-hepa and hiPSC-hepa have drug metabolism capacity. Furthermore, hESC-hepa and hiPSC-hepa were examined to determine whether these cells may be applied to evaluate drug-induced cytotoxicity.

Materials and methods

In vitro differentiation

Before the initiation of cellular differentiation, the medium of hESCs and hiPSCs was exchanged for a defined serum-free medium, hESF9, and cultured as previously reported [9]. The differentiation protocol for the induction of DE cells, hepatoblasts, and hepatocytes was based on our previous report with some modifications [5,6]. Briefly, in mesendoderm differentiation, hESCs and hiPSCs were dissociated into single cells by using Accutase (Millipore) and cultured for 2 days on Matrigel (BD biosciences) in differentiation hESF-DIF medium which contains 100 ng/ml Activin A (R&D Systems) and 10 ng/ml bFGF (hESF-DIF medium, Cell Science & Technology Institute; differentiation hESF-DIF medium was supplemented with 10 μg/ml human recombinant insulin, 5 μg/ml human apotransferrin, 10 μM 2-mercaptoethanol, 10 μM ethanolamine, 10 μM sodium selenite, and 0.5 mg/ml bovine serum albumin, all from Sigma). To generate DE cells, mesendoderm cells were transduced with 3000 VP/cell of Ad-FOXA2 for 1.5 h on day 2 and cultured until day 6 on Matrigel in differentiation hESF-DIF medium supplemented with 100 ng/ml Activin A and 10 ng/ml bFGF. For induction of hepatoblasts, the DE cells were transduced with each 1500 VP/cell of Ad-FOXA2 and Ad-HNF1α for 1.5 h on day 6 and cultured for 3 days on Matrigel in hepatocyte culture medium (HCM, Lonza) supplemented with 30 ng/ml bone morphogenetic protein 4 (BMP4, R&D Systems) and 20 ng/ml FGF4 (R&D Systems). In hepatic expansion, the hepatoblasts were transduced with each 1500 VP/cell of Ad-FOXA2 and Ad-HNF1α for 1.5 h on day 9 and cultured for 3 days on Matrigel in HCM supplemented with 10 ng/ml hepatocyte growth factor (HGF), 10 ng/ml FGF1, 10 ng/ml FGF4, and 10 ng/ml FGF10 (all from R&D Systems). In hepatic maturation, cells were cultured for 8 days on Matrigel in L15 medium (Invitrogen) supplemented with 8.3% tryptose phosphate broth (BD biosciences), 10% FBS (Vita), 10 μM hydrocortisone 21-hemisuccinate (Sigma), 1 μM insulin, 25 mM $NaHCO_3$ (Wako), 20 ng/ml HGF, 20 ng/ml Oncostatin M (OsM, R&D systems), and 10^{-6} M Dexamethasone (DEX, Sigma).

Results

Recently, we showed that the sequential transduction of SOX17, HEX, and HNF4α into hESC-derived mesendoderm, DE, and hepatoblasts, respectively, leads to efficient generation of the hESC-hepa [5–7]. In the present study, to further improve the differentiation efficiency towards hepatocytes, we screened for hepatic differentiation-promoting transcription factors. Seven candidate genes involved in liver development were selected. We then examined the function of the hESC-hepa and hiPSC-hepa generated by the optimized protocol for pharmaceutical use in detail.

Efficient hepatic differentiation by Ad-FOXA2 and Ad-HNF1α transduction

To perform efficient DE differentiation, T-positive hESC-derived mesendoderm cells (day 2) (Supplementary Fig. 1) were transduced with Ad vector expressing various transcription factors (Ad-FOXA2, Ad-HEX, Ad-HNF1α, Ad-HNF1β, Ad-HNF4α, Ad-HNF6, and Ad-SOX17 were used in this study). We ascertained the expression of *FOXA2*, *HEX*, *HNF1α*, *HNF1β*, *HNF4α*, *HNF6*, or *SOX17* in Ad-FOXA2-, Ad-HEX-, Ad-HNF1α-, Ad-HNF1β-, Ad-HNF4α-, Ad-HNF6-, or Ad-SOX17-transduced cells, respectively (Supplementary Fig. 2). We also verified that there was no cytotoxicity of the cells transduced with Ad vector until the total amount of Ad vector reached 12,000 VP/cell (Supplementary Fig. 3). Each transcription factor was expressed in hESC-derived mesendoderm cells on day 2 by using Ad vector, and the efficiency of DE differentiation was examined (Fig. 1A). The DE differentiation efficiency based on CXCR4-positive cells was the highest when Ad-SOX17 or Ad-FOXA2 were transduced (Fig. 1B). To investigate the difference between Ad-FOXA2-transduced cells and Ad-SOX17-transduced cells, gene expression levels of markers of undifferentiated cells, mesendoderm cells, DE cells, and extraembryonic endoderm cells were examined (Fig. 1C). The expression levels of extraembryonic endoderm markers of Ad-SOX17-transduced cells were higher than those of Ad-FOXA2-transduced cells. Therefore, we concluded that FOXA2 transduction is suitable for use in selective DE differentiation.

To promote hepatic commitment, various transcription factors were transduced into DE cells and the resulting phenotypes were examined on day 9 (Fig. 1D). Nearly 100% of the population of Ad-FOXA2-transduced cells and Ad-HNF1α-transduced cells was α-fetoprotein (AFP)-positive (Fig. 1E). We expected that hepatic commitment would be further accelerated by combining FOXA2 and HNF1α transduction. The DE cells were transduced with both Ad-FOXA2 and Ad-HNF1α, and then the gene expression levels of *CYP3A7* [10], which is a marker of fetal hepatocytes, were evaluated (Fig. 1F). When both Ad-FOXA2 and Ad-HNF1α were transduced into DE cells, the promotion of hepatic commitment was greater than in Ad-FOXA2-transduced cells or Ad-HNF1α-transduced cells.

To promote hepatic expansion and maturation, we transduced various transcription factors into hepatoblasts on day 9 and 12 and the resulting phenotypes were examined on day 20 (Fig. 1G). We ascertained that the hepatoblast population was efficiently expanded by addition of HGF, FGF1, FGF4, and FGF10 (Supplementary Fig. 4). The hepatic differentiation efficiency based on asialoglycoprotein receptor 1 (ASGR1)-positive cells was measured on day 20, demonstrating that FOXA2, HNF1α, and HNF4α transduction could promote efficient hepatic maturation (Fig. 1H). To investigate the phenotypic difference between Ad-FOXA2-, Ad-HNF1α-, and Ad-HNF4α-transduced cells, gene expression levels of early hepatic markers, mature hepatic markers, and biliary markers were examined (Fig. 1I). Gene expression levels of mature hepatic markers were up-regulated by FOXA2, HNF1α, or HNF4α transduction. FOXA2 transduction strongly upregulated gene expression levels of both early hepatic markers and mature hepatic markers, while HNF1α or HNF4α transduc-

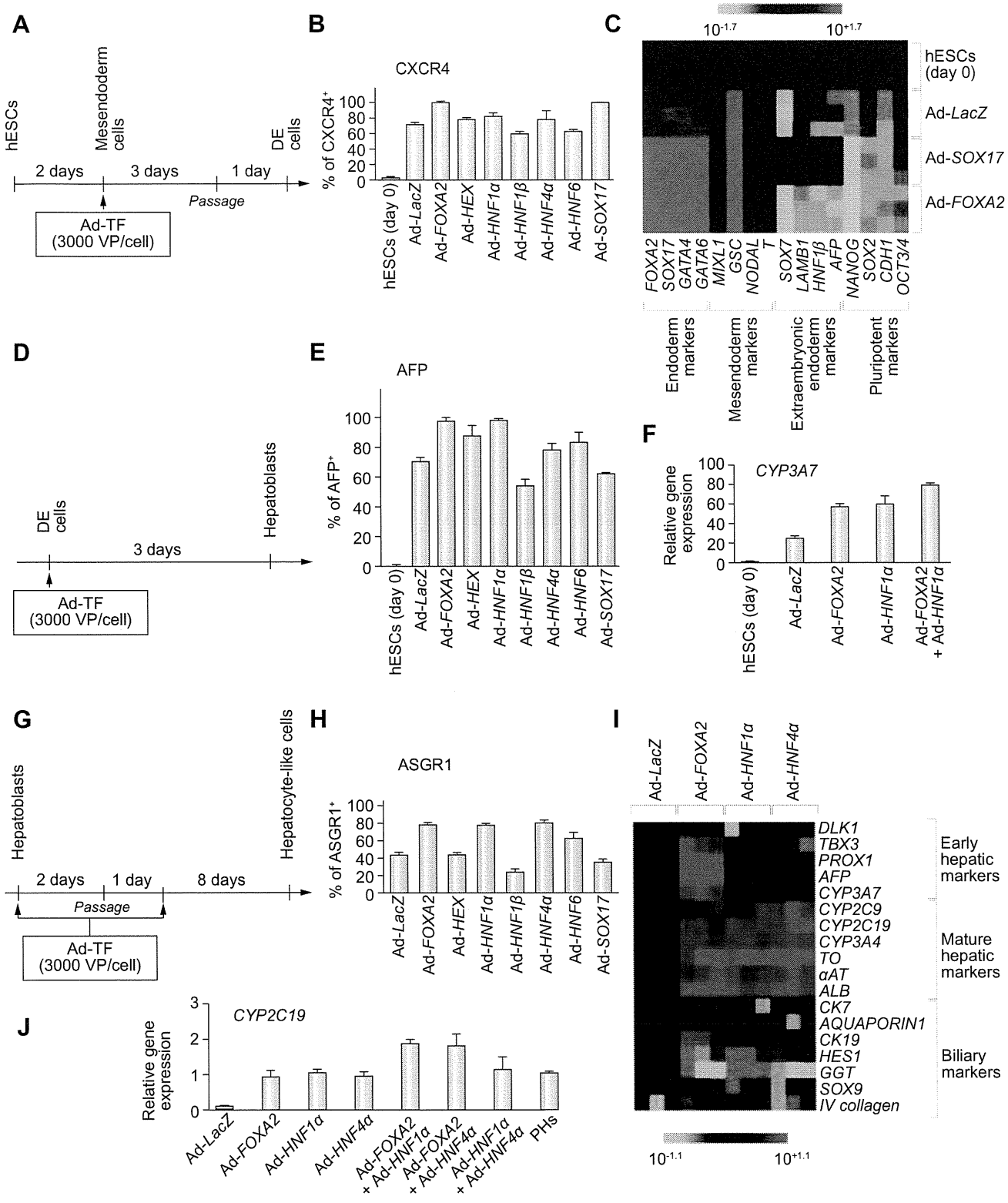

Fig. 1. Efficient hepatic differentiation from hESCs by FOXA2 and HNF1α transduction. (A) The schematic protocol describes the strategy for DE differentiation from hESCs (H9). Mesendoderm cells (day 2) were transduced with 3000 VP/cell of transcription factor (TF)-expressing Ad vector (Ad-TF) for 1.5 h and cultured as described in Fig. 2A. (B) On day 5, the efficiency of DE differentiation was measured by estimating the percentage of CXCR4-positive cells using FACS analysis. (C) The gene expression profiles were examined on day 5. (D) Schematic protocol describing the strategy for hepatoblast differentiation from DE. DE cells (day 6) were transduced with 3000 VP/cell of Ad-TF for 1.5 h and cultured as described in Fig. 2A. (E) On day 9, the efficiency of hepatoblast differentiation was measured by estimating the percentage of AFP-positive

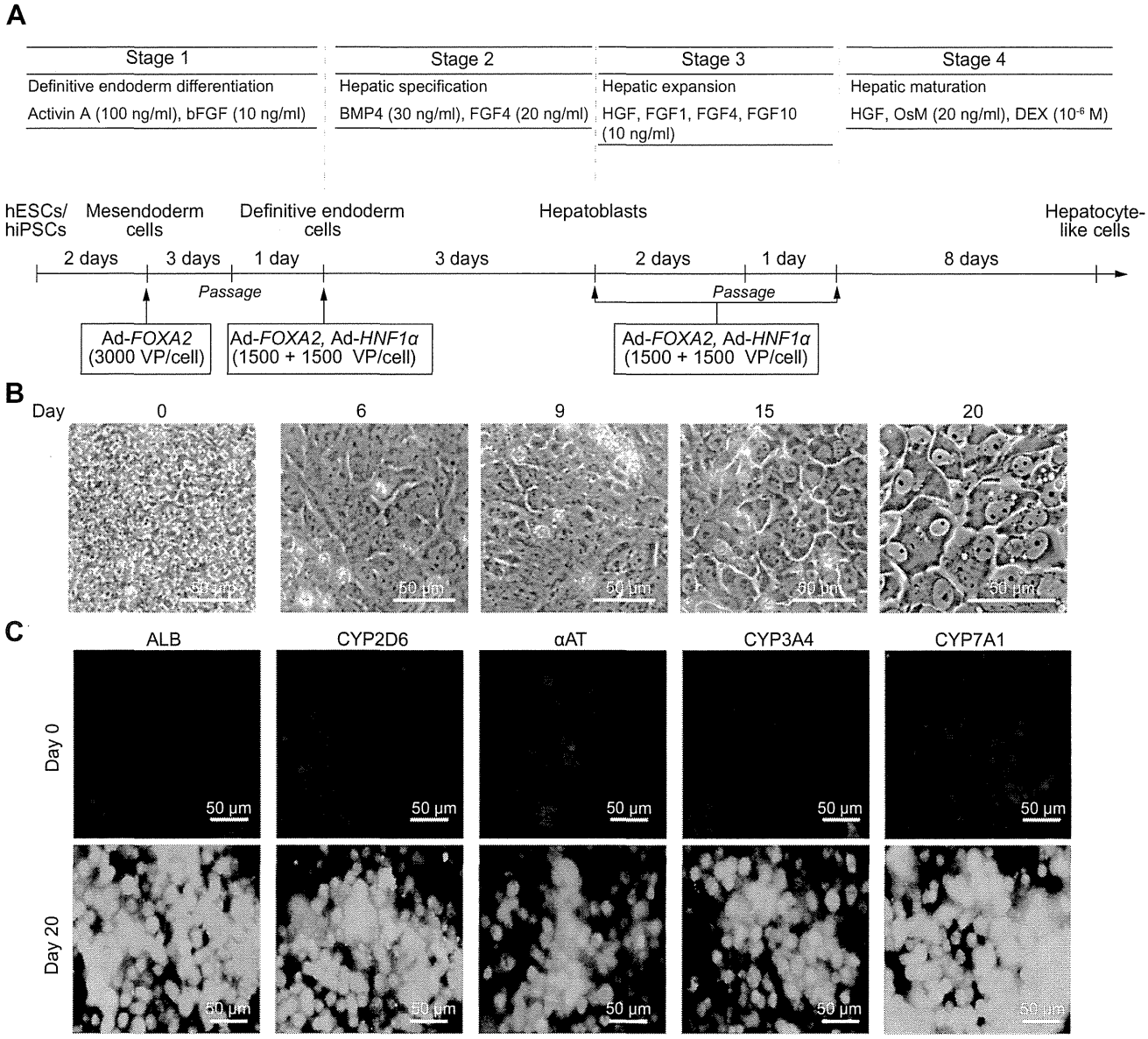

Fig. 2. Hepatic differentiation of hESCs and hiPSCs by FOXA2 and HNF1α transduction. (A) The differentiation procedure of hESCs and hiPSCs into hepatocytes via DE cells and hepatoblasts is schematically shown. Details of the hepatic differentiation procedure are described in Materials and methods. (B) Sequential morphological changes (day 0–20) of hESCs (H9) differentiated into hepatocytes are shown. (C) The expression of the hepatocyte markers (ALB, CYP2D6, αAT, CYP3A4, and CYP7A1, all green) was examined by immunohistochemistry on day 0 and 20. Nuclei were counterstained with DAPI (blue).

tion did not up-regulate the gene expression levels of early hepatic markers. Next, multiple transduction of transcription factors was performed to promote further hepatic maturation. The combination of Ad-FOXA2 and Ad-HNF1α transduction and the combination of Ad-FOXA2 and Ad-HNF4α transduction result in the most efficient hepatic maturation, judged from the gene expression levels of *CYP2C19* (Fig. 1J). This may happen because the mixture of immature hepatocytes and mature hepatocytes coor-

cells using FACS analysis. (F) The gene expression level of *CYP3A7* was measured by real-time RT-PCR on day 9. On the *y* axis, the gene expression level of *CYP3A7* in hESCs (day 0) was taken as 1.0. (G) The schematic protocol describes the strategy for hepatic differentiation from hepatoblasts. Hepatoblasts (day 9) were transduced with 3000 VP/cell of Ad-TF for 1.5 h and cultured as described in Fig. 2A. (H) On day 20, the efficiency of hepatic differentiation was measured by estimating the percentage of ASGR1-positive cells using FACS analysis. The detail results of FACS analysis are shown in Supplementary Table 1. (I) Gene expression profiles were examined on day 20. (J) Hepatoblasts (day 9) were transduced with 3000 VP/cell of Ad-TFs (in the case of combination transduction of two types of Ad vector, 1500 VP/cell of each Ad-TF was transduced) for 1.5 h and cultured. Gene expression levels of *CYP2C19* were measured by real-time RT-PCR on day 20. On the *y* axis, the gene expression level of *CYP2C19* in PHs, which were cultured for 48 h after the cells were plated, was taken as 1.0. All data are represented as mean ± SD (n = 3).

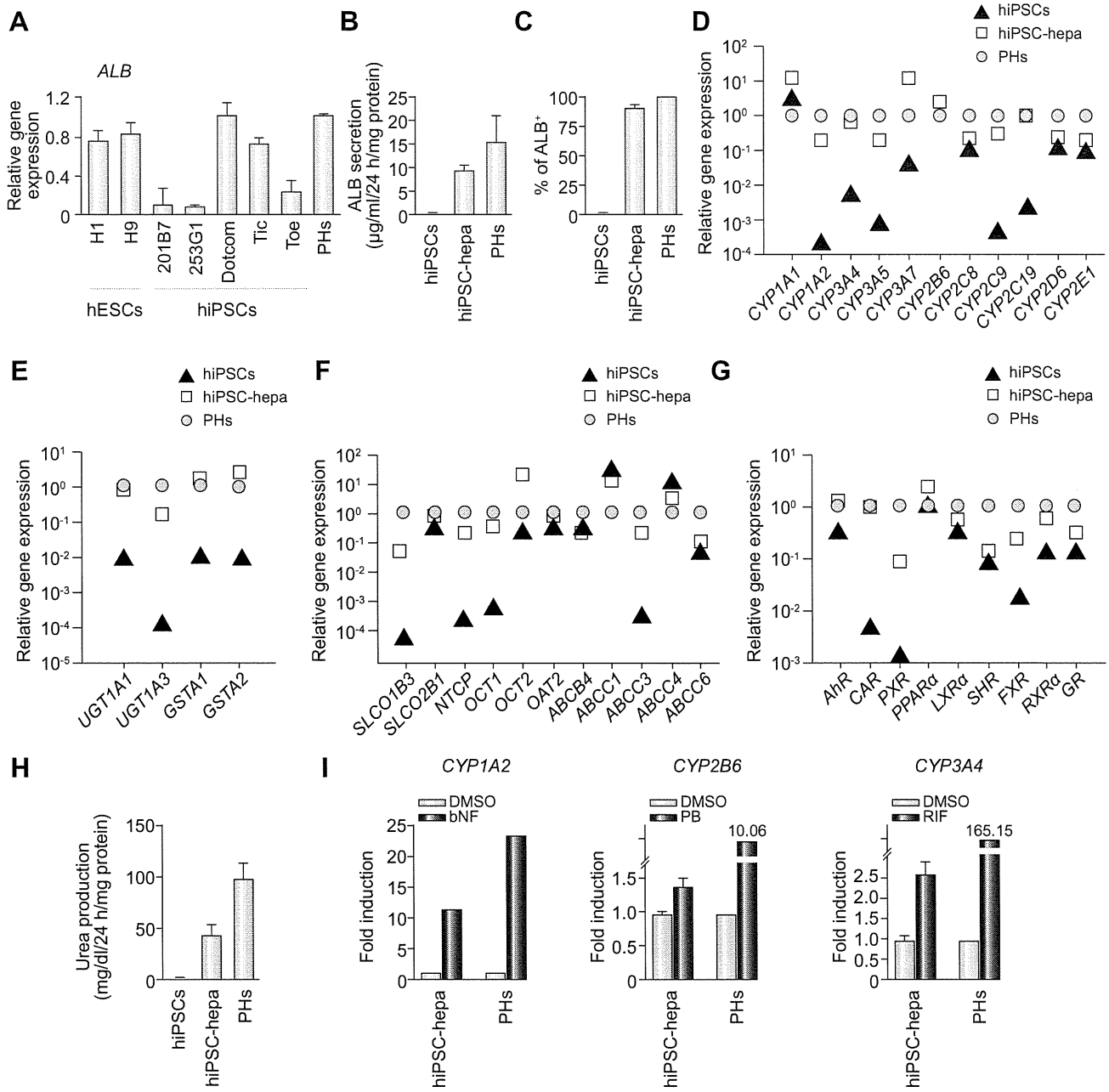

Fig. 3. The hepatic characterization of hiPSC-hepa. hESCs (H1 and H9) and hiPSCs (201B7, 253G1, Dotcom, Tic, and Toe) were differentiated into hepatocyte-like cells as described in Fig. 2A. (A) On day 20, the gene expression level of *ALB* was examined by real-time RT-PCR. On the *y* axis, the gene expression level of *ALB* in PHs, which were cultured for 48 h after cells were plated, was taken as 1.0. (B–I) hiPSCs (Dotcom) were differentiated into hepatocyte-like cells as described in Fig. 2A. (B) The amount of ALB secretion was examined by ELISA in hiPSCs, hiPSC-hepa, and PHs. (C) hiPSCs, hiPSC-hepa, and PHs were subjected to immunostaining with anti-ALB antibodies, and then the percentage of ALB-positive cells was examined by flow cytometry. (D–G) The gene expression levels of CYP enzymes (D), conjugating enzymes (E), hepatic transporters (F), and hepatic nuclear receptors (G) were examined by real-time RT-PCR in hiPSCs, hiPSC-hepa, and PHs. On the *y* axis, the expression level of PHs is indicated. (H) The amount of urea secretion was examined in hiPSCs, hiPSC-hepa, and PHs. (I) Induction of *CYP1A2*, *2B6*, or *3A4* by DMSO or inducer (bNF, PB, or RIF) of hiPSC-hepa and PHs, cultured for 48 h after the cells were plated, was examined. On the y axis, the gene expression levels of *CYP1A2*, *2B6*, or *3A4* in DMSO-treated cells, which were cultured for 48 h, were taken as 1.0. All data are represented as mean ± SD (n = 3).

dinately works to induce hepatocyte functions. Taken together, efficient hepatic differentiation could be promoted by using the combination of FOXA2 and HNF1α transduction at the optimal stage of differentiation (Fig. 2A). At the stage of hepatic expansion and maturation, Ad-HNF4α can be substituted for Ad-HNF1α (Fig. 1J). Interestingly, cell growth was delayed by FOXA2 and HNF4α transduction (Supplementary Fig. 5). This delay in cell proliferation might be due to promoted maturation by FOXA2 and HNF1α transduction. As the hepatic differentiation proceeds, the morphology of hESCs gradually changed into a typical hepatocyte morphology, with distinct round nuclei and a polygonal shape (Fig. 2B), and the expression levels of hepatic markers

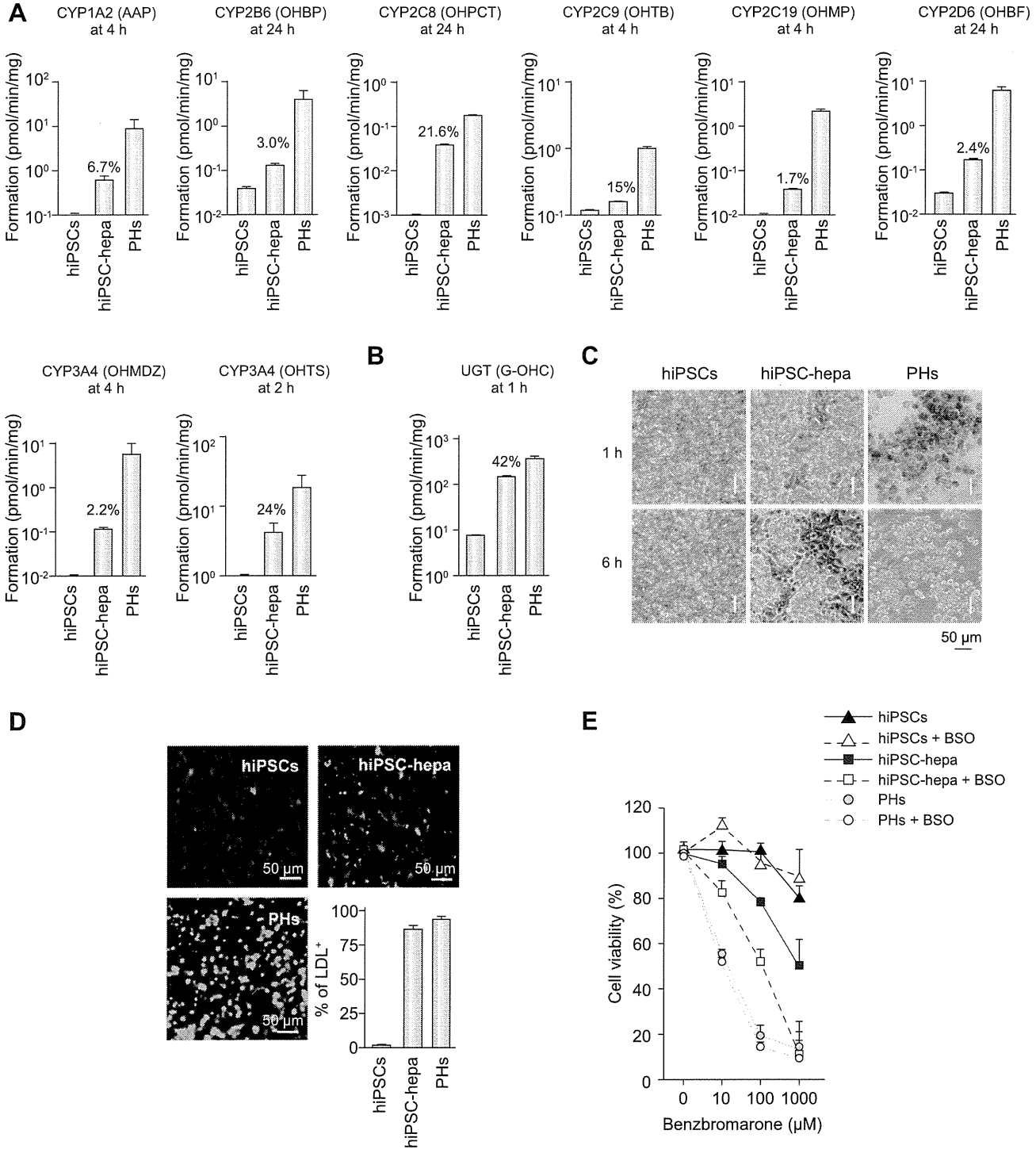

Fig. 4. Evaluation of the drug metabolism capacity and hepatic transporter activity of hiPSC-hepa. hiPSCs (Dotcom) were differentiated into hepatocytes as described in Fig. 2A. (A and B) Quantitation of metabolites in hiPSCs, hiPSC-hepa, and PHs, which were cultured for 48 h after the cells were plated, was examined by treating nine substrates (Phenacetin, Bupropion, Paclitazel, Tolbtamide, *S*-mephenytoin, Bufuralol, Midazolam, Testosterone, and Hydroxyl coumarin; these compounds are substrates for CYP1A2, 2B6, 2C8, 2C9, 2C19, 2D6, 3A4, 3A4 (A) and UGT (B), respectively), and then supernatants were collected at the indicated time. The quantity of metabolites (Acetaminophen [AAP], Hydroxybupropion [OHBP], 6α-hydroxypaclitaxel [OHPCT], Hydroxytolbutamide [OHTB], 4′-hydroxymephenytoin [OHMP], 1′-hydroxybufuralol [OHBF], 1′-hydroxymidazolam [OHMDZ], 6β-hydroxytestosterone [OHTS], 7-Hydroxycoumarin glucuronide [G-OHC], respectively) was measured by LC-MS/MS. The ratios of the activity levels in hiPSC-hepa to the activity levels in PHs rate are indicated in the graph. (C) hiPSCs, hiPSC-hepa, and PHs were examined for their ability to take up ICG (top) and release it 6 h thereafter (bottom). (D) hiPSCs, hiPSC-hepa, and PHs were cultured with medium containing Alexa-Flour 488-labeled LDL (green) for 1 h, and immunohistochemistry was performed. Nuclei were counterstained with DAPI (blue). The percentage of LDL-positive cells was also measured by FACS analysis. (E)

(ALB, CYP2D6, alpha-1-antitrypsin [αAT], CYP3A4, and CYP7A1) increased (Fig. 2C). Hepatic gene expression levels (Supplementary Fig. 6A), amount of ALB secretion (Supplementary Fig. 6B), and CYP2C9 activity level (Supplementary Fig. 6C) of Ad-FOXA2- and Ad-HNF1α-transduced cells were significantly higher than those of Ad-SOX17-, Ad-HEX-, and Ad-HNF4α-transduced cells. These results indicated that FOXA2 and HNF1α transduction promotes more efficiently hepatic differentiation than SOX17, HEX, and HNF4α transduction.

Characterization of the hESC-hepa/hiPSC-hepa

As we have previously reported [6], hepatic differentiation efficiency differs among hESC/hiPSC lines. Therefore, it is necessary to select a hESC/hiPSC line that is suitable for hepatic maturation in the case of medical applications such as drug screening. In the present study, two hESC lines and five hiPSCs lines were differentiated into hepatocyte-like cells, and then their gene expression levels of *ALB* (Fig. 3A) and *CYP3A4* (Supplementary Fig. 7A), and their CYP3A4 activities (Supplementary Fig. 7B) were compared. These data suggest that the iPSC line, Dotcom [11,12], was the most suitable for hepatocyte maturation. To examine whether the iPSC (Dotcom)-hepa has enough hepatic functions as compared with PHs, the amount of albumin (ALB) secretion (Fig. 3B) and the percentage of ALB-positive cells (Fig. 3C) were measured on day 20. The amount of ALB secretion in hiPSC-hepa was similar to that in PHs and the percentage of ALB-positive cells was approximately 90% in iPSC-hepa. We also confirmed that the gene expression levels of CYP enzymes (Fig. 3D), conjugating enzymes (Fig. 3E), hepatic transporters (Fig. 3F), and hepatic nuclear receptors (Fig. 3G) in hiPSC-hepa were similar to those of PHs, although some of them were still lower than those of PHs. Because the gene expression level of the fetal CYP isoform, *CYP3A7*, in hiPSC-hepa was higher than that of PHs, mature hepatocytes and hepatic precursors were still mixed. We have previously confirmed that Ad vector-mediated gene expression in the hepatoblasts (day 9) continued until day 14 and almost disappeared on day 18 [7]. Therefore, the hepatocyte-related genes expressed in hiPSC-hepa are not directly regulated by exogenous FOXA2 or HNF1α. Taken together, endogenous hepatocyte-related genes in hiPSC-hepa should have been upregulated by FOXA2 and HNF1α transduction.

To further confirm that hiPSC-hepa have sufficient levels of hepatocyte functions, we evaluated the ability of urea secretion (Fig. 3H) and glycogen storage (Supplementary Fig. 8). The amount of urea secretion in hiPSC-hepa was about half of that in PHs. HiPSC-hepa exhibited abundant storage of glycogen. Because CYP1A2, 2B6, and 3A4 are involved in the metabolism of a significant proportion of the currently available commercial drugs, we tested the induction of *CYP1A2*, *2B6*, and *3A4* by chemical stimulation (Fig. 3I). *CYP1A2*, *2B6*, and *3A4* are induced by β-naphthoflavone [bNF], phenobarbital [PB], or rifampicin [RIF], respectively. Although undifferentiated hiPSCs did not respond to either bNF, PB, or RIF (data not shown), hiPSC-hepa produced more metabolites in response to chemical stimulation, suggesting that inducible CYP enzymes were detectable in hiPSC-hepa (Fig. 3I). However, the induction potency of *CYP1A2*, *2B6*, and *3A4* in hiPSC-hepa were lower than that in PHs.

Drug metabolism capacity and hepatic transporter activity of hiPSC-hepa

Because metabolism and detoxification in the liver are mainly executed by CYP enzymes, conjugating enzymes, and hepatic transporters, it is important to assess the function of these enzymes and transporters in hiPSC-hepa. Among the various enzymes in liver, CYP1A2, 2B6, 2C8, 2C9, 2C19, 2D6 and 3A4, UGT are the important phase I and II enzymes responsible for metabolism. Nine substrates, Phenacetin, Bupropion, Paclitazel, Tolbtamide, *S*-mephenytoin, Bufuralol, Midazolam, Testosterone, and Hydroxyl coumarin, which are the substrates of CYP1A2, 2B6, 2C8, 2C9, 2C19, 2D6, 3A4, 3A4 (Fig. 4A), and UGT (Fig. 4B), respectively, were used to estimate the drug metabolism capacity of hiPSC-hepa compared with that of PHs. To precisely estimate the drug metabolism capacity, the amounts of metabolites were measured during the phase when production of metabolites was linear (Supplementary Fig. 9). These results indicated that our hiPSC-hepa have the capacity to metabolize these nine substrates, although the activity levels were lower than those of PHs. The hepatic functions of hiPSC-hepa were further evaluated by examining the ability to uptake Indocyanine Green (ICG) and LDL (Fig. 4C and D, respectively). In addition to PHs, hiPSC-hepa had the ability to uptake ICG and to excrete ICG in a culture without ICG for 6 h (Fig. 4C), and to uptake LDL (Fig. 4D). These results suggest that hiPSC-hepa have enough CYP enzyme activity, conjugating enzyme activity, and hepatic transporter activity to metabolize various drugs.

To examine whether our hiPSC-hepa could be used to predict metabolism-mediated toxicity, hiPSC-hepa were incubated with Benzbromarone, which is known to generate toxic metabolites, and then cell viability was measured (Fig. 4E). Cell viability of hiPSC-hepa was decreased depending on the concentration of Benzbromarone. However, cell viability of hiPSC-hepa was much higher than that of PHs. To detect drug-induced cytotoxicity with high sensitivity in hiPSC-hepa, these cells were treated with Buthionine-SR-sulfoximine (BSO), which depletes cellular GST, and result in a decrease of cell viability of hiPSC-hepa as compared with that of non-treated cells (Fig. 4E). These results indicated that hiPSC-hepa would be more useful in drug screening under a condition of knockdown of conjugating enzyme activity.

Discussion

The establishment of an efficient hepatic differentiation technology from hESCs and hiPSCs would be important for the application of hESC-hepa and hiPSC-hepa to drug toxicity screening. Although we have previously reported that sequential transduc-

The cell viability of hiPSCs, hiPSC-hepa, PHs, and their BSO-treated cells (0.4 mM BSO was pre-treated for 24 h) was assessed by Alamar Blue assay after 48-hr exposure to differe2nt concentrations of benzbromarone. The cell viability is expressed as a percentage of that in cells treated only with solvent. All data are represented as mean ± SD (n = 3).

tion of SOX17, HEX, and HNF4α into hESC-derived cells could promote efficient hepatic differentiation [7], further hepatic maturation of the hESC-hepa and hiPSC-hepa was needed for this application. To further improve the differentiation efficiency of every step of hepatic differentiation (hESC to DE cells, DE cells to hepatoblasts, and hepatoblasts to hESC-hepa), we initially performed a screening of transcription factors. In the stage of DE differentiation, FOXA2 transduction could promote the most efficient DE differentiation (Fig. 1C). In the stage of hepatic commitment, expansion, and maturation, the combination of FOXA2 and HNF1α transduction strongly promoted hepatic commitment and maturation (Fig. 1F and J), although in the stage of hepatic expansion and maturation, HNF4α transduction was as efficient as that of HNF1α (Fig. 1J). Since HNF1α is one of the target genes of HNF4α [13], the signaling through HNF4α to HNF1α would be important for efficient hepatic expansion and maturation. Considering these results together, we ascertained a pair of two transcription factors, FOXA2 and HNF1α, that could promote efficient hepatic differentiation from hESCs. In embryogenesis, the expression of FOXA2 and HNF1α is initially detected in DE or hepatoblasts, respectively and the expression levels of both FOXA2 and HNF1α are elevated as the liver develops [14,15]. Therefore, our hepatic differentiation technology, which employs FOXA2 and HNF1α transduction, might mimic the gene expression pattern during embryogenesis.

We found that the gene expression levels of CYP enzymes, conjugating enzymes, hepatic transporters, and hepatic nuclear receptors were upregulated by FOXA2 and HNF1α transduction (Fig. 3D–G). In contrast to the high expression levels of hepatocyte-related genes, CYP induction potency and the drug metabolism capacity of our hiPSC-hepa were lower than those of PHs (Figs. 3I and 4A and B). One of the possible reasons for the difference between gene expression levels of CYP enzymes and CYP induction activity might be that there were insufficient expression levels of hepatic nuclear receptors (such as *PXR*, *SHR*, and *FXR*) in hiPSC-hepa (Fig. 3G). Because many CYPs require high expression levels of hepatic nuclear receptor for efficient drug metabolism [16], transduction of these hepatic nuclear receptor genes in hiPSC-hepa or development of a differentiation method that induces high expression of these nuclear receptors might improve the drug metabolic capacity. Another explanation for the low CYP activities in hiPSC-hepa, maybe that hiPSCs were established from an individual with low CYP activities; infact, it is known that large individual differences in CYP activities are observed among individuals. It might be important to use a hiPSC line established from a person with high CYP activities. It is essential to investigate the reasons behind this significant discordance, an issue that our group is currently planning to study.

In summary, our method, consisting of sequential FOXA2 and HNF1α transduction along with the addition of adequate soluble factors at each step of differentiation, is a valuable tool for the efficient generation of functional hepatocytes derived from hESCs and hiPSCs. The hiPSC-hepa exhibited a number of hepatocyte functions (such as ALB secretion, uptake of LDL or ICG, glycogen storage, and drug metabolism capacity). In addition, the hiPSC-hepa were successfully applied to the evaluation of drug-induced cytotoxicity. Therefore, the hESC-hepa and hiPSC-hepa might be used for drug screening in early phases of pharmaceutical development.

Conflict of interest

The authors who have taken part in this study declared that they do not have anything to disclose regarding funding or conflict of interest with respect to this manuscript.

Acknowledgements

We thank Misae Nishijima, Nobue Hirata, Miki Yoshioka, and Hiroko Matsumura for their excellent technical support. We thank Ms. Ong Tyng Tyng for critical reading of the manuscript. HM, MKF, and TH were supported by grants from the Ministry of Health, Labor, and Welfare of Japan. HM was also supported by Japan Research foundation For Clinical Pharmacology, The Nakatomi Foundation, and The Uehara Memorial Foundation. K. Kawabata was supported by Grants from the Ministry of Education, Sports, Science and Technology of Japan (20200076) and the Ministry of Health, Labor, and Welfare of Japan. K. Katayama and FS were supported by Program for Promotion of Fundamental Studies in Health Sciences of the National Institute of Biomedical Innovation (NIBIO).

Supplementary data

Supplementary data associated with this article can be found, in the online version, at http://dx.doi.org/10.1016/j.jhep.2012.04.038.

References

[1] Thomson JA, Itskovitz-Eldor J, Shapiro SS, Waknitz MA, Swiergiel JJ, Marshall VS, et al. Embryonic stem cell lines derived from human blastocysts. Science 1998;282:1145–1147.
[2] Takahashi K, Tanabe K, Ohnuki M, Narita M, Ichisaka T, Tomoda K, et al. Induction of pluripotent stem cells from adult human fibroblasts by defined factors. Cell 2007;131:861–872.
[3] Clayton DF, Darnell Jr JE. Changes in liver-specific compared to common gene transcription during primary culture of mouse hepatocytes. Mol Cell Biol 1983;3:1552–1561.
[4] Snykers S, De Kock J, Rogiers V, Vanhaecke T. In vitro differentiation of embryonic and adult stem cells into hepatocytes: state of the art. Stem cells 2009;27:577–605.
[5] Inamura M, Kawabata K, Takayama K, Tashiro K, Sakurai F, Katayama K, et al. Efficient generation of hepatoblasts from human ES cells and iPS cells by transient overexpression of homeobox gene HEX. Mol Ther 2011;19:400–407.
[6] Takayama K, Inamura M, Kawabata K, Tashiro K, Katayama K, Sakurai F, et al. Efficient and directive generation of two distinct endoderm lineages from human ESCs and iPSCs by differentiation stage-specific SOX17 transduction. PLoS One 2011;6:e21780.
[7] Takayama K, Inamura M, Kawabata K, Katayama K, Higuchi M, Tashiro K, et al. efficient generation of functional hepatocytes from human embryonic stem cells and induced pluripotent stem cells by HNF4alpha transduction. Mol Ther 2012;20:127–137.
[8] Duan Y, Ma X, Zou W, Wang C, Bahbahan IS, Ahuja TP, et al. Differentiation and characterization of metabolically functioning hepatocytes from human embryonic stem cells. Stem cells 2010;28:674–686.
[9] Furue MK, Na J, Jackson JP, Okamoto T, Jones M, Baker D, et al. Heparin promotes the growth of human embryonic stem cells in a defined serum-free medium. Proc Natl Acad Sci U S A 2008;105:13409–13414.
[10] Lacroix D, Sonnier M, Moncion A, Cheron G, Cresteil T. Expression of CYP3A in the human liver–evidence that the shift between CYP3A7 and CYP3A4 occurs immediately after birth. Eur J Biochem 1997;247:625–634.

[11] Nagata S, Toyoda M, Yamaguchi S, Hirano K, Makino H, Nishino K, et al. Efficient reprogramming of human and mouse primary extra-embryonic cells to pluripotent stem cells. Genes Cells 2009;14:1395–1404.
[12] Makino H, Toyoda M, Matsumoto K, Saito H, Nishino K, Fukawatase Y, et al. Mesenchymal to embryonic incomplete transition of human cells by chimeric OCT4/3 (POU5F1) with physiological co-activator EWS. Exp Cell Res 2009;315:2727–2740.
[13] Gragnoli C, Lindner T, Cockburn BN, Kaisaki PJ, Gragnoli F, Marozzi G, et al. Maturity-onset diabetes of the young due to a mutation in the hepatocyte nuclear factor-4 alpha binding site in the promoter of the hepatocyte nuclear factor-1 alpha gene. Diabetes 1997;46:1648–1651.
[14] Ang SL, Wierda A, Wong D, Stevens KA, Cascio S, Rossant J, et al. The formation and maintenance of the definitive endoderm lineage in the mouse: involvement of HNF3/forkhead proteins. Development 1993;119: 1301–1315.
[15] Kyrmizi I, Hatzis P, Katrakili N, Tronche F, Gonzalez FJ, Talianidis I. Plasticity and expanding complexity of the hepatic transcription factor network during liver development. Genes Dev 2006;20:2293–2305.
[16] Lehmann JM, McKee DD, Watson MA, Willson TM, Moore JT, Kliewer SA. The human orphan nuclear receptor PXR is activated by compounds that regulate CYP3A4 gene expression and cause drug interactions. J Clin Invest 1998;102:1016–1023.

Biomaterials 33 (2012) 4526–4534

Contents lists available at SciVerse ScienceDirect

Biomaterials

journal homepage: www.elsevier.com/locate/biomaterials

The promotion of hepatic maturation of human pluripotent stem cells in 3D co-culture using type I collagen and Swiss 3T3 cell sheets

Yasuhito Nagamoto [a,b], Katsuhisa Tashiro [b], Kazuo Takayama [a,b], Kazuo Ohashi [d], Kenji Kawabata [b,c], Fuminori Sakurai [a], Masashi Tachibana [a], Takao Hayakawa [e,f], Miho Kusuda Furue [g,h], Hiroyuki Mizuguchi [a,b,i,*]

[a] Laboratory of Biochemistry and Molecular Biology, Graduate School of Pharmaceutical Sciences, Osaka University, Osaka 565-0871, Japan
[b] Laboratory of Stem Cell Regulation, National Institute of Biomedical Innovation, Osaka 567-0085, Japan
[c] Laboratory of Biomedical Innovation, Graduate School of Pharmaceutical Sciences, Osaka University, Osaka 565-0871, Japan
[d] Institute of Advanced Biomedical Engineering and Science, Tokyo Women's Medical University, Tokyo 162-8666, Japan
[e] Pharmaceutics and Medical Devices Agency, Tokyo 100-0013, Japan
[f] Pharmaceutical Research and Technology Institute, Kinki University, Osaka 577-8502, Japan
[g] Laboratory of Cell Cultures, Department of Disease Bioresources, National Institute of Biomedical Innovation, Osaka 567-0085, Japan
[h] Laboratory of Cell Processing, Institute for Frontier Medical Sciences, Kyoto University, Kyoto 606-8507, Japan
[i] The Center for Advanced Medical Engineering and Informatics, Osaka University, Osaka 565-0871, Japan

ARTICLE INFO

Article history:
Received 16 February 2012
Accepted 3 March 2012
Available online 23 March 2012

Keywords:
Hepatocyte
Co-culture
Collagen
Fibroblast
Liver
ECM (extracellular matrix)

ABSTRACT

Hepatocyte-like cells differentiated from human embryonic stem cells (hESCs) or human induced pluripotent stem cells (hiPSCs) are known to be a useful cell source for drug screening. We recently developed an efficient hepatic differentiation method from hESCs and hiPSCs by sequential transduction of FOXA2 and HNF1α. It is known that the combination of three-dimensional (3D) culture and co-culture, namely 3D co-culture, can maintain the functions of primary hepatocytes. However, hepatic maturation of hESC- or hiPSC-derived hepatocyte-like cells (hEHs or hiPHs, respectively) by 3D co-culture systems has not been examined. Therefore, we utilized a cell sheet engineering technology to promote hepatic maturation. The gene expression levels of hepatocyte-related markers (such as cytochrome P450 enzymes and conjugating enzymes) and the amount of albumin secretion in the hEHs or hiPHs, which were 3D co-cultured with the Swiss 3T3 cell sheet, were significantly up-regulated in comparison with those in the hEHs or hiPHs cultured in a monolayer. Furthermore, we found that type I collagen synthesized in Swiss 3T3 cells plays an important role in hepatic maturation. The hEHs or hiPHs that were 3D co-cultured with the Swiss 3T3 cell sheet would be powerful tools for medical applications, such as drug screening.

1. Introduction

Several studies have recently shown the ability of human embryonic stem cells (hESCs) [1] and human induced pluripotent stem cells (hiPSCs) [2] to differentiate into hepatocyte-like cells [3–6]. Although primary human hepatocytes are generally employed for drug toxicity screening in the early phase of pharmaceutical development, these cells have some drawbacks, such as their limited range of sources, difference in variability and functions from batch to batch, and de-differentiation. Because hESC- or hiPSC-derived hepatocyte-like cells (hEHs or hiPHs, respectively) have potential to resolve these problems, they are expected to be applied to drug screening. The hepatic differentiation processes from hESCs and hiPSCs are divided into three-stages, differentiation into definitive endoderm (DE) cells, hepatoblasts, and mature hepatocytes. Hepatic differentiation methods based on the treatment of growth factors have been widely used to generate hepatocyte-like cells from hESCs or hiPSCs [5–9]. However, the hepatic differentiation efficiency is not high enough for medical applications such as drug screening [10]. To promote the efficiency of hepatic differentiation and hepatic maturation, we have developed hepatic differentiation methods that combine the transduction of transcription factor genes involved in liver development

* Corresponding author. Laboratory of Biochemistry and Molecular Biology, Graduate School of Pharmaceutical Sciences, Osaka University, 1-6 Yamadaoka, Suita, Osaka 565-0871, Japan. Tel.: +81 6 6879 8185; fax: +81 6 6879 8186.
E-mail address: mizuguch@phs.osaka-u.ac.jp (H. Mizuguchi).

0142-9612/$ – see front matter © 2012 Elsevier Ltd. All rights reserved.
doi:10.1016/j.biomaterials.2012.03.011

with stimulation by growth factors [11–13]. The hepatocyte-like cells generated by our protocols have levels of expression of hepatocyte-related genes similar to the levels in (cryopreserved) primary human hepatocytes cultured for 48 h after plating [12]. Moreover, we have recently established more efficient and simple methods for hepatic differentiation from hESCs and hiPSCs by sequential transduction of forkhead box A2 (FOXA2) and hepatocyte nuclear factor 1 homeobox A (HNF1α) (in submitted). In that recent study, we showed that the hEHs or hiPHs expressed the genes of hepatocyte-related markers at levels similar to those in primary human hepatocytes and could metabolize various types of drugs.

It is known that cell–cell interactions between hepatocytes and their surrounding cells are essential for liver development and maintenance of liver functions [14–17]. Although primary human hepatocytes rapidly lose their functions under a monolayer culture condition, they could retain their functions, such as albumin secretion and urea synthesis, in three-dimensional (3D) culture and co-culture [18–21]. Moreover, it has been reported that the primary hepatocytes maintain their functions for a long time by the combination of 3D culture and co-culture, namely 3D co-culture [22–24]. In particular, the functions of primary rat hepatocytes cultured in a 3D co-culture, were shown to be more efficiently preserved than the functions of primary rat hepatocytes cultured in monolayer a co-culture [24]. Recently, Kim et al. reported that primary rat hepatocytes are able to maintain their functions in 3D co-culture with an endothelial cell sheet [25]. To perform 3D co-culture with a cell sheet, they employed cell sheet engineering technology using temperature-responsive culture dishes grafted with a temperature-responsive polymer, poly(*N*-isopropylacrylamide). This cell sheet engineering technology make it possible to manipulate a monolayer cell sheet with the extracellular matrices (ECMs) synthesized from the cells [26]. Although 3D culture or co-culture methods have been individually applied to promote hepatic differentiation from ESCs or iPSCs [27–29], few studies have investigated the hepatic differentiation from hESCS or hiPSCs using a 3D co-culture method.

In this study, we examined whether 3D co-culture, which uses the cell sheet engineering technology, could promote hepatic differentiation, and particularly the differentiation into mature hepatocyte-like cells, from hESCs and hiPSCs. Because Swiss 3T3 cells are widely used for co-culture with primary hepatocytes [18–20], we employed Swiss 3T3 cells for 3D co-culture with the hEHs or hiPHs. After hEHs and hiPHs were 3D co-cultured with a Swiss 3T3 cell sheet, we examined the expression levels of hepatocyte-related genes. Moreover, we investigated a Swiss 3T3 cell-derived factor that can promote hepatic maturation from hESCs and hiPSCs.

2. Materials and methods

2.1. hESC and hiPSC culture

A hESC line, H9 (WiCell Research Institute), was maintained on a feeder layer of mitomycin C (MMC)-treated mouse embryonic fibroblasts (MEF, Millipore) with ReproStem (ReproCELL) supplemented with 5 ng/ml fibroblast growth factor 2 (FGF2) (Sigma). hESCs were dissociated with 0.1 mg/ml dispase (Roche Diagnostics) into small clumps and were then subcultured every 4 or 5 days. H9 cells were was used following the Guidelines for Derivation and Utilization of Human Embryonic Stem Cells of the Ministry of Education, Culture, Sports, Science and Technology of Japan. One hiPSC line generated from the human embryonic lung fibroblast cell line MCR5 was provided from the JCRB Cell Bank (Tic, JCRB Number: JCRB1331). Another hiPSC line, 201B7, generated from human dermal fibroblasts was kindly provided by Dr. S. Yamanaka (KyotoUniversity). These hiPSC lines were maintained on a feeder layer of MMC-treated MEF with iPSellon (for Tic, Cardio) or ReproStem (for 201B7, ReproCELL) supplemented with 10 ng/ml (for Tic) or 5 ng/ml (for 201B7) FGF2.hiPSCs were dissociated with 0.1 mg/ml dispase (Roche Diagnostics) into small clumps and were then subcultured every 5 or 6 days.

2.2. Swiss 3T3 cell culture

A mouse fibroblast line, Swiss 3T3, was maintained with RPMI-1640 medium (Sigma) supplemented with fetal bovine serum (10%) (FBS), streptomycin (120 μg/ml), and penicillin (200 μg/ml).

2.3. Ad vectors

The human eukaryotic translation elongation factor 1 alpha 1 (EF-1α) promoter-driven HNF1α- and FOXA2-expressing Ad vectors (Ad-HNF1α and Ad-FOXA2, respectively) were constructed previously (in submitted). All of Ad vectors contain a stretch of lysine residue (K7) peptides in the C-terminal region of the fiber knob for more efficient transduction of hESCs, hiPSCs, and DE cells, in which transduction efficiency was almost 100%, and purified as described previously [11,12,30]. The vector particle (VP) titer was determined by using a spectrophotometric method [31].

2.4. In vitro differentiation

Before the initiation of cellular differentiation, the medium of hESCs and hiPSCs was exchanged for a defined serum-free medium, hESF9, and hESCs and hiPSCs were cultured as previously reported [32]. The differentiation protocol for the induction of DE cells, hepatoblasts, and hepatocytes was based on our previous report with some modifications (in submitted). Briefly, in mesendoderm differentiation, hESCs and hiPSCs were dissociated into single cells by using Accutase (Millipore) and cultured for 2 days on Matrigel (BD Biosciences) in hESF-DIF medium (Cell Science & Technology Institute) supplemented with 10 μg/ml human recombinant insulin, 5 μg/ml human apotransferrin, 10 μM 2-mercaptoethanol, 10 μM ethanolamine, 10 μM sodium selenite, and 0.5 mg/ml bovine serum albumin (BSA) (all from Sigma) (differentiation hESF-DIF medium) containing 100 ng/ml Activin A (R&D Systems) and 10 ng/ml FGF2. To generate DE cells, hESC- or hiPSC-derived mesendoderm cells were transduced with 3000 VP/cell of Ad-FOXA2 for 1.5 h on day 2 and cultured until day 6 on Matrigel in differentiation hESF-DIF medium supplemented with 100 ng/ml Activin A and 10 ng/ml FGF2. For induction of the hepatoblasts, the hESC- or hiPSC-derived DE cells were transduced with each 1500 VP/cell of Ad-FOXA2 and Ad-HNF1α for 1.5 h on day 6 and cultured for 3 days on Matrigel in hepatocyte culture medium (HCM) (Lonza) supplemented with 30 ng/ml bone morphogenetic protein 4 (BMP4) and 20 ng/ml FGF4 (all from R&D Systems). To expand the hepatoblasts, the hepatoblasts were transduced with each 1500 VP/cell of Ad-FOXA2 and Ad-HNF1α for 1.5 h on day 9 and cultured for 3 days on Matrigel in HCM supplemented with 10 ng/ml hepatocyte growth factor (HGF), 10 ng/ml FGF1, 10 ng/ml FGF4, and 10 ng/ml FGF10 (all from R&D Systems).To induce hepatic maturation, the cells were cultured for 2 days on Matrigel in L15 medium (Invitrogen) supplemented with 8.3% tryptose phosphate broth (BD Biosciences), 10% FBS (Vita), 10 μM hydrocortisone 21-hemisuccinate (Sigma), 1 μM insulin, and 25 mM NaHCO3 (Wako) (differentiation L15 medium) containing 20 ng/ml hepatocyte growth factor (HGF), 20 ng/ml Oncostatin M (OsM) (R&D Systems), and 10^{-6} M Dexamethasone (DEX) (Sigma). As described below, the Swiss 3T3 cell sheet was stratified onto hepatocyte-like cells on day 14 and cultured in differentiation L15 medium supplemented with 20 ng/ml HGF, 20 ng/ml OsM, and 10^{-6} M DEX until day 15. On day 15, Matrigel was stratified onto the cells and cultured in differentiation L15 medium supplemented with 20 ng/ml HGF, 20 ng/ml OsM, and 10^{-6} M DEX until day 25.

2.5. Cell sheet harvesting and stratifying procedure utilizing a gelatin-coated manipulator

The stratifying protocol was performed as previously described with some modifications [25,33]. Briefly, Swiss 3T3 cells were seeded on a 24-well temperature-responsive culture plate (TRCP) (Cell Seed Inc, Tokyo) on day 12. Two days after seeding (day 14), Swiss 3T3 cells were grown to confluence. On the same day (day 14), a gelatin-coated cell sheet manipulator was placed on the Swiss 3T3 cells, and the culture temperature was reduced to 20 °C for 60 min. By removing the manipulator, cultured Swiss 3T3 cells were harvested as a contiguous cell sheet that attached on the gelatin. The Swiss 3T3 cell sheet was then stratified on the hEHs or hiPHs. The culture plate with the manipulator was incubated at room temperature for 60 min to induce adherence between the hEHs or hiPHs and Swiss 3T3 cell sheet. To dissolve the gelatin, the culture plate was incubated at 37 °C for 60 min, and this was followed by several washing steps.

2.6. RNA isolation and reverse transcription-PCR

Total RNA was isolated from the hESC- or hiPSC-derived cells using ISOGENE (Nippon Gene) according to the manufacturer's instructions. cDNA was synthesized using 500 ng of total RNA with a Superscript VILO cDNA synthesis kit (Invitrogen). Real-time RT-PCR was performed with Taqman gene expression assays or Fast SYBR Green Master Mix using an ABI Step One Plus (all from Applied Biosystems). Relative quantification was performed against a standard curve and the values were normalized against the input determined for the housekeeping gene, *glyceraldehyde 3-phosphate dehydrogenase* (*GAPDH*). The primer sequences used in this study are described in Supplementary Tables 1 and 2.

2.7. Preparation of verticalsection

On day 15, the hEHs cultured with or without the Swiss 3T3 cell sheet were frozen in Tissue-Tek O.C.T. Compound (Sakura Finetek), then vertically sectioned and fixed with 4% paraformaldehyde. These sections were monitored by a phase contrast microscope (Olympus).

2.8. ELISA

hESCs or hiPSCs were differentiated into the hepatocyte-like cells as described in Fig. 1A. The culture supernatants, which were incubated for 24 h after fresh medium was added, were collected and analyzed to determine the amount of ALB secretion by ELISA. ELISA kits for ALB were purchased from Bethyl Laboratories. ELISA was performed according to the manufacturer's instructions. The amount of ALB secretion was calculated according to each standard.

2.9. Co-culture and culture in a cell culture insert system (insert-culture)

hESCs were differentiated into the hepatocyte-like cells as described in Fig. 1A until day 14, and then the hESC-derived cells were harvested and seeded onto a 6-well culture plate (Falcon) with Swiss 3T3 (1:1) in a co-culture system. In a insert-culture system, hESC-derived hepatocyte-like cells were harvested and seeded onto a 6-well culture plate alone, and Swiss 3T3 cells were plated in cell culture inserts (membrane pore size 1.0 μm; Falcon), and placed in a well of the culture palate containing hESC-derived hepatocyte-like cells. These cells were cultured in differentiation L15 medium supplemented with 20 ng/ml HGF, 20 ng/ml OsM, and 10^{-6} M DEX until day 25.

2.10. Stratification of type I collagen gel

A type I collagen gel solution was prepared as suggested by Nitta Gelatin: 7 parts of solubilized collagen in HCl (pH 3.0) 2 parts of 5× concentrated RPMI-1640 medium, and 2 parts of reconstitution buffer (0.2 M HEPES, 0.08 M NaOH) to neutralize the collagen gel, were mixed gently but rapidly at 4 °C. Next, the hESC-derived cells were cultured in a type I collagen gel solution for 3h, and then the medium waschanged and the cells were cultured in differentiation L15 medium supplemented with 20 ng/ml HGF, 20 ng/ml OsM, and 10^{-6} M DEX until day 25.

2.11. Inhibition of collagen synthesis

hESCs were differentiated into the hepatocyte-like cells as described in Fig. 1A until stratification of the Swiss 3T3 cell sheet. After stratification of the Swiss 3T3 cell sheet, the cells were cultured in differentiation L15 medium supplemented with 20 ng/ml HGF, 20 ng/ml OsM, 10^{-6} M DEX, and 25 μM 2,2′-Bipyridyl (Wako), an inhibitor of collagen synthesis, until day 25.

2.12. Western blotting analysis

Swiss 3T3 cells were cultured with 25 μM 2,2′-Bipyridyl or solvent (0.1% DMSO) for 3 days, and these cells were then homogenized with lysis buffer (1% Nonidet P-40, 1 mM EDTA, 25 mM Tris-HCl, 5 mM NaF, and 150 mM NaCl) containing protease inhibitor mixture (Sigma-Aldrich). After being frozen and thawed, the homogenates were centrifuged at 15,000× *g* at 4 °C for 10 min, and the supernatants were collected. The lysates were subjected to SDS-PAGE on 7.5% polyacrylamide gel and were then transferred onto polyvinylidene fluoride membranes (Millipore). After the reaction was blocked with 1% skim milk in TBS containing 0.1% Tween 20 at room temperature for 1 h, the membranes were incubated with goat anti-col1a1 Ab (diluted 1/200; Santa Cruz Biotechnology) or mouse anti-β-actin Ab (diluted 1/5000; Sigma) at 4 °C overnight, followed by reaction with horseradish peroxidase-conjugated anti-goat IgG (Chemicon) or anti-mouse IgG (Cell Signaling Technology) at room temperature for 1 h. The band was visualized by ECL Plus Western blotting detection reagents (GE Healthcare) and the signals were read using a LAS-3000 imaging system (FUJI Film).

2.13. Statistical analysis

Statistical analysis was performed using the unpaired two-tailed Student's *t*-test.

3. Results

3.1. Efficient hepatic maturation by stratification of the Swiss 3T3 cell sheet

The hEHs, which were generated by the transduction of *HNF1α* and *FOXA2* genes, were 3D co-cultured with the Swiss 3T3 cell sheet to promote hepatic differentiation and to generate mature hepatocytes from hESCs and hiPSCs. Our differentiation strategy using the stratification of the Swiss 3T3 cell sheet is illustrated in Fig. 1A. The stratifying procedure was performed on day 14 as described in Fig. 1B. The day after stratifying the Swiss 3T3 cell sheet on the hEHs, vertical sections of the monolayer hEHs (hEHs-mono) and the hEHs stratified with the Swiss 3T3 cell sheet (hEHs-Swiss) were prepared (Fig. 1C). We found that Swiss 3T3 cells were successfully harvested and overlaid onto the hEHs as a monolayer cell sheet (Fig. 1C). Moreover, the hEHs seemed to be larger than the Swiss 3T3 cells. The space between the hEHs cells and Swiss 3T3 cells suggests the formation of ECMs (Fig. 1C).

To investigate whether stratification of the Swiss 3T3 cell sheet could promote hepatic maturation of the hEHs, hESCs (H9) were differentiated into the hepatocyte-like cells according to the protocol described in Fig. 1A, and then the gene expression levels of hepatocyte-related markers and the amount of albumin (ALB) secretion in the hEHs-Swiss were measured on day 25 (Fig. 2). By 3D co-culturing of the hepatocyte-like cells with the Swiss 3T3 cell sheet for 10 days (days 15–25), the gene expression levels of hepatocyte-related markers, such as *ALB* (Fig. 2A), *hepatocyte nuclear factor 4 alpha* (*HNF4A*) (Fig. 2B), cytochrome P450 (CYP) enzymes (*CYP2C9*, *CYP7A1*, *CYP1A2*, and *CYP3A5*) (Fig. 2D–G), and conjugating enzymes (*glutathione S-transferase alpha 1* [*GSTA1*], *GSTA2*, and *UDP glucuronosyltransferase* [*UGT1A1*]) (Fig. 2H–J) were significantly increased as compared with those in hEHs-mono. Moreover, the amount of ALB secretion in hEHs-Swiss was also up-regulated as compared with that in hEHs-mono (Fig. 2K). Because it is known that hepatoblasts can differentiate into hepatocytes and cholangiocytes [34,35], we examined the gene expression level of *cytokeratin 7* (*CK7*), a cholangiocyte-related marker, in hEHs-Swiss and hEHs-mono. In 3D co-culture with the Swiss 3T3 cell sheet, the gene expression level of *CK7* was down-regulated in the hEHs-Swiss relative to the hEHs-mono (Fig. 2C). These results clearly showed that stratification of the Swiss 3T3 cell sheet could promote the hepatic maturation of the hEHs and, in turn, suppress the cholangiocyte differentiation.

In order to investigate whether stratification of the Swiss 3T3 cell sheet promotes maturation of hiPHs as well as hEHs, the hiPSCs (Tic and 201B7) were differentiated into the hepatocyte-like cells according to the protocol described in Fig. 1A. The results showed that the gene expression levels of *ALB*, *CYP2C9*, *CYP3A5*, *CYP1A2*, and *GSTA1* in the hiPHs stratified with the Swiss 3T3 cell sheet (hiPHs-Swiss) were up-regulated in comparison with those in the monolayer hiPHs (hiPHs-mono) (Fig. 3A–E). Moreover, the gene expression level of *CK7* was markedly decreased in hiPHs-Swiss (Fig. 3F). The gene expression level of *ALB* in the hiPHs-Swiss differentiated from Tic was higher than that in the hiPHs-Swiss differentiated from 201B7, while the gene expression levels of CYP enzymes in the hiPHs-Swiss differentiated from Tic were lower than those in the hiPHs-Swiss differentiated from 201B7 (Fig. 3A–D). These results showed that stratification of the Swiss 3T3 cell sheet promoted hepatic maturation of both hEHs and hiPHs.

3.2. Identification of maturation factors synthesized from Swiss 3T3 cells

The data described above indicate that hepatic maturation factors were produced in Swiss 3T3 cells. To elucidate the Swiss 3T3 cell-derived hepatic maturation factors, the hEHs were cultured in cell culture-insert systems (insert-cultured), in which the hEHs were co-cultured with Swiss 3T3 cells without physical contacts, or co-cultured with Swiss 3T3 cells. Quantitative PCR analysis revealed that the gene expression levels of *ALB* and *CYP2C9* in the insert-cultured hEHs were increased in comparison with the hEHs-mono, while the expression levels of these genes were lower than